Computers and Electronics in Agriculture 232 (2025) 110134

Contents lists available at ScienceDirect

Computers and Electronics in Agriculture

journal homepage: www.elsevier.com/locate/compag

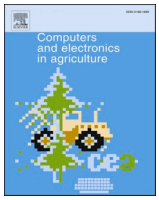

Optimizing the regeneration of spruce-dominated stands suffering from Heterobasidion root rot in Finland

Eero Holmström [a,*], Juha Honkaniemi [a], Anssi Ahtikoski [a], Tuomas Rajala [a], Jarkko Hantula [a], Tuula Piri [a], Juha Heikkinen [a], Susanne Suvanto [a], Tapio Räsänen [b], Juha-Antti Sorsa [b], Kirsi Riekki [b], Henna Höglund [c], Aleksi Lehtonen [a], Mikko Peltoniemi [a]

[a] Natural Resources Institute Finland (Luke), Latokartanonkaari 9, 00790 Helsinki, Finland
[b] Metsäteho Oy, Vernissakatu 1, 01300 Vantaa, Finland
[c] Finnish Forest Centre, Olavinkatu 60, 57100 Savonlinna, Finland

ARTICLE INFO

Keywords:
Heterobasidion root rot
Precision forestry
Microstand
Harvester data
Disease control
Forest planning
Stand dynamics
Bayesian modeling

ABSTRACT

Heterobasidion root rot is a destructive fungal disease causing extensive damage in conifer forests throughout the Northern hemisphere. The effective spreading of the causal agent *Heterobasidion* sp. from one tree generation to the next makes the disease a persistent problem for forestry. Here, we present a precision-forestry method for optimizing the regeneration of spruce-dominated stands suffering from Heterobasidion root rot. Our method prevents the inter-generational spread of the disease while aiming for high financial or climate change mitigation value. The method uses harvester data with non-parametric clustering or Bayesian modeling to delineate the stand into healthy and infected "microstands." Through simulations of forest growth and *Heterobasidion* dynamics, the optimal species to plant in each microstand to maximize either bare land value (BLV, interest rate 2%) or net CO_2 removals by living tree biomass is determined, subject to the condition that regeneration leads to disease eradication. In Finnish conditions, the method recommends pine on mesic heath sites (MT) and combinations of pine and spruce on herb-rich sites (OMT) to maximize BLV. To maximize CO_2 removals, the method suggests a variety of tree species compositions including birch. In comparison to regenerating using only spruce, the predicted mean financial gain from the method is 1320 ± 40 EUR/ha on MT and 400 to 800 EUR/ha on OMT. Direct gains in CO_2 removals are difficult to achieve due to prevailing management practices for infected stands. The method offers financial and carbon-wise support for decision-making while diversifying forests and cleansing sites of root rot disease.

1. Introduction

Heterobasidion root rot is a destructive fungal disease that causes extensive damage to conifer forests throughout the Northern Hemisphere (Korhonen and Stenlid 1998, Garbelotto and Gonthier 2013). The disease causes annual losses estimated to exceed 1200 MEUR within the EU only (Woodward et al. 1998). In Norway spruce (*Picea abies L.* Karst.), the dominant causal agent in Finland is *H. parviporum* Niemelä & Korhonen (Piri et al. 1990), which can infect only species of genus *Picea* and *Larix* in Finland. The more generalist causal agent *H. annosum* s.s., which infects also *Pinus* sp. and many other species, is less common in the southern parts of Finland, but may infect spruce especially at former pine sites (Korhonen 1978). *H. parviporum* is the most common root rot causing agent in Southern Finland and becomes less common as one moves northwards (Korhonen and Piri 1994), whereas *H. annosum* s.s. is concentrated in the pine-dominated areas of Eastern Finland.

In a spruce tree infected by *H. parviporum*, the fungus grows from the root system to the stem base and further upwards into the stem, with the decay column reaching as high as 10 to 12 m in mature trees (Stenlid and Wästerlund 1986). As the fungus grows along the stem, sawlog-quality spruce wood is degraded to pulp or energy grade. In addition, Heterobasidion root rot makes infected forest stands less resistant to wind

* Corresponding author.
E-mail addresses: eero.holmstrom@luke.fi (E. Holmström), juha.honkaniemi@luke.fi (J. Honkaniemi), anssi.ahtikoski@luke.fi (A. Ahtikoski), tuomas.rajala@luke.fi (T. Rajala), jarkko.hantula@gmail.com (J. Hantula), ext.tuula.piri@luke.fi (T. Piri), juha.heikkinen@luke.fi (J. Heikkinen), susanne.suvanto@luke.fi (S. Suvanto), tapio.rasanen@metsateho.fi (T. Räsänen), juha-antti.sorsa@metsateho.fi (J.-A. Sorsa), kirsi.riekki@metsateho.fi (K. Riekki), henna.hoglund@metsakeskus.fi (H. Höglund), aleksi.lehtonen@luke.fi (A. Lehtonen), mikko.peltoniemi@luke.fi (M. Peltoniemi).

https://doi.org/10.1016/j.compag.2025.110134
Received 26 August 2024; Received in revised form 12 February 2025; Accepted 13 February 2025
Available online 21 February 2025

damage and other forest disturbances (Oliva et al. 2008, Honkaniemi et al. 2018, Wahlman 2024). Moreover, climate change mitigation via forest use is rendered less effective, with short-lived forest products being produced instead of long-term products, and forest stands acting as carbon storages with reduced stability.

H. parviporum spreads through two mechanisms, of which the first is primary infection through airborne spores that land on stumps or wounds in trees, colonizing stumps and eventually the roots. In addition, *H. parviporum* spreads through secondary infections by vegetative growth of mycelium along roots. This enables the fungus to spread from the roots of an infected stump or tree to the overlapping roots of neighboring spruce trees, leading to new infections both within and between tree generations (Möykkynen and Pukkala 2011, Honkaniemi et al. 2017). The warming climate will increase the spread of root rot disease, at least in boreal conditions (Müller et al. 2015).

Treating freshly cut stumps with urea or the biological control fungus *Phlebiopsis gigantea*, or performing harvesting operations during wintertime in the Nordic countries, are effective and established ways of preventing the onset of new primary infections of *H. parviporum*. However, preventing secondary infections between tree generations has turned out a far more difficult problem to solve.

In a stand infected by *H. parviporum*, after a clearcut, the fungus will continue to live in large spruce stumps for as long as 40 to 50 years (Piri 1996). When a stand is being regenerated, if spruce is planted into the infected regions of the stand, the new generation of trees will become infected via the secondary infection mechanism. Different approaches to preventing infections between tree generations have been tested over the years. These include the removal of infected stumps and roots, or the uprooting of infected trees along with one row of healthy trees and the subsequent digging of deep trenches, these being approaches with limited practical appeal due to high expenses, negative environmental impacts, or the increased risk of primary infections (Garbelotto and Gonthier 2013). The most successful approach to date has been changing the tree species. Birch (*Betula* sp.) and pine (*Pinus sylvestris L.*) are resistant to *H. parviporum*. Planting these species into the diseased areas of a felled stand can be used to purify the stand of root rot (Korhonen 1978, Piri 2003, Möykkynen and Pukkala 2011). During one rotation period, the infected stumps decompose, and *H. parviporum* is eradicated from the site. This however requires, that naturally regenerated spruce saplings are removed from the stand, as these sustain the disease (Piri and Korhonen 2001, Möykkynen and Pukkala 2011). In the healthy parts of the stand, one can plant a new generation of spruce trees.

Regenerating a spruce-dominated stand infected by *H. parviporum* through changing the tree species should provide several benefits. First, getting rid of root rot disease could help to restore financial losses associated with the disease in spruce trees. Second, growing healthy spruce trees instead of diseased ones supports climate change mitigation through producing sawlogs instead of pulp or energy wood and through making stands more resistant to other disturbances. Third, considering alternative species to spruce, in particular broad-leaved trees, can boost the biodiversity of forests as well as climate-change adaptation measures and the resistance of forests to a wide range of natural disturbances (Griess and Knoke 2011, Pretzsch et al. 2013, Jactel et al. 2017).

So far, the main problem of implementing optimal forest management practices based on changing tree species within infected stands has been the lack of information on root rot distribution in forests. Detecting Heterobasidion root rot based on visual appearance of standing trees is not possible. However, immediately after felling the trees, root rot can be detected from the cut surfaces with relatively high confidence (except when the infection is recent and limited to the root system). When recorded during the harvesting process, this presents a valuable source of information which could be used to guide stand regeneration and planting – and eventually root-rot eradication – in a precision-forestry approach of managing infected forests at a scale finer than the stand level (Holopainen et al. 2014).

Simulation studies by Aza et al. (2022) using such tree-level infection data in a precision-forestry framework suggest that in grid cells of low infection levels within a stand, planting spruce is a profitable option, whereas in cells of high infection levels, it is financially beneficial to use pine. More recently, Lara et al. (2024) leveraged harvester-based rot data to study the clustering of spruce trees suffering from root rot. The authors suggested planting alternative tree species around individual infected stumps within a radius dependent on the cluster size to disrupt the inter-generational spread of root rot via vegetative growth. However, end-to-end precision-forestry methods for eradicating root rot disease while optimizing stand productivity have been missing thus far. These types of methods could be implemented in technical solutions that operationalize harvester data for pathogen eradication and forest management optimization. This would require considering a wide range of forest management options including tree species mixtures, as well as assessing CO_2 sequestration and requiring disease eradication when designing management plans.

In this work, we present a novel, open-source, precision-forestry optimization pipeline for planning the regeneration of spruce stands suffering from root rot caused by *H. parviporum*. The goal of the method is to maximize either the bare land value (BLV) or net CO_2 removals by the living tree biomass of the stand, under the requirement that the stand is purified of root rot, i.e., the disease is eradicated from the site. At the core of our approach is the segmentation of the processed stand into microstands which delineate the healthy and infected regions of the stand, based on either known disease centers as found directly from harvester data, or using Bayesian modeling to predict future infection risk within the stand. Via simulations of tree growth and *Heterobasidion* dynamics, our method finds the optimal choice of tree species to plant in each region of the stand, including the possibility of mixtures. By applying our method on a validation dataset of recently harvested stands, we study the distributions of the produced tree species recommendations, estimate the expected benefits of the optimization, and find whether purely financially optimal forest regeneration can be used to eradicate root rot from infected stands. Finally, we discuss the implications and practical considerations of taking our method into operational use as well as directions for future work.

2. Materials and methods

In this section, we first give a general description of the optimization method in Section 2.1. After this, we present each stage of the method in more detail in Sections 2.2-2.6. Finally, we describe the dataset and computations used to assess the optimization method in Section 2.7.

2.1. Overview of the optimization method

The purpose of our optimization method is to help the forest owner plan the regeneration of their stand in such a way that the stand is purified of root rot disease and high economic or climate change mitigation value is obtained. To accomplish this, we built a method pipeline consisting of the following steps. The pipeline is graphically presented in Fig. 1.

First, a root rot detection algorithm is applied to the cut-to-length harvester data describing how the spruce stems were cut into logs, i.e., bucked during the final felling of the stand. This harvester data is stored in the StanForD 2010 HPR format. The analysis results in a binary rot indicator (healthy, rotten) for each harvested spruce stem. The rot detection algorithm is described in more detail in Section 2.2.

Next, the stand is split into healthy and infected regions, i.e., "microstands," based on the rot data on the harvested stems. We provide two alternative approaches to this, the first of which is density-based clustering of the rotten stump positions. The second, more involved approach, is to use Bayesian modeling to estimate the size and shape of the effective root systems of rotten spruce trees, and to utilize this information to predict the future risk of infection within the stand. The process of splitting a stand into microstands through these two

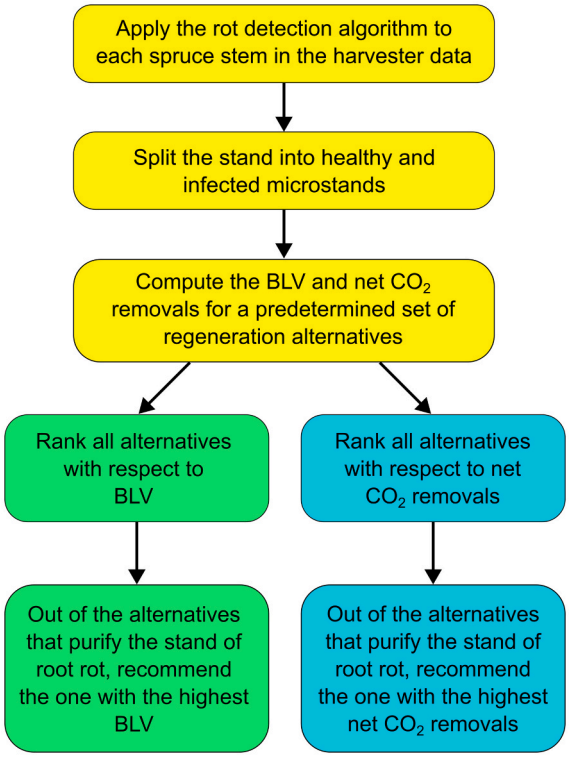

Fig. 1. The structure of the optimization pipeline.

approaches is described in more detail in Section 2.3.

Then, considering a set of 10 different regeneration alternatives, the total BLV, i.e., the financial result for each alternative is computed as the sum of the BLVs of the healthy and infected microstands. In addition, for each alternative, the sum of the maximum attainable net CO_2 removals by the living tree biomass during one rotation period, i.e., the maximum of the time series of the net CO_2 removals, is computed over the microstands for each of the regeneration alternatives. The BLV and the CO_2 computations for each alternative are based on simulations of forest growth and *Heterobasidion* dynamics. The different regeneration alternatives and their rationale are described in Section 2.4. The simulations are described in Section 2.5, and the calculation of BLV and CO_2 removals is described in Section 2.6.

Finally, two recommendations for regenerating a given stand are produced from the preceding analysis (Fig. 1). First, the different regeneration alternatives are ranked according to BLV. Out of those alternatives where the stand is purified of root rot, the one with the highest BLV is presented as the regeneration recommendation. Then, the regeneration alternatives are ranked according to net CO_2 removals. Out of those alternatives where the stand is purified of root rot, the one giving the highest CO_2 removals is presented as the regeneration recommendation. The forest owner may choose from these two recommendations based on their preference, guided by expert evaluation and certain practical considerations (Section 4).

The optimization code, which requires the stand data including the rot status of the harvested spruce trees as input, is called *regenopt*. It has been written in Python 3 and is available at https://doi.org/10.5281/zenodo.13132120. The code for performing the Bayesian modeling is available as the R package *latentsn* at https://doi.org/10.5281/zenodo.13269316.

2.2. The root rot detection algorithm

The forest harvester records the bucking performed on each stem into the StanForD 2010 HPR file. For each processed stem, the created logs are recorded starting from the stem base, and for each log, at least the length, top diameter, volume, and log assortment are recorded. The harvester bucking automation suggests to the machine operator at which points to cross-cut the stem into logs. The operator can deviate from this automated suggestion and choose the cutting point independently. This is done especially because of defects and other quality-related reasons.

Our algorithm for detecting root rot on spruce stems is based on the interpretation of the log assortment and the location of the log on the stem. In its simplest form, root rot detection can be summed up by the question: has anything other than sawlogs been cut from the butt-end of the sawlog-sized stem? More specifically, we adopt the following criterion for labeling a felled spruce stem as suffering from root rot disease: If no sawlog has been cut from the butt end of the sawlog-sized stem for a distance of two meters, and at least one sawlog was produced from the stem, the stem is assumed to have root rot. This definition reflects the fact that for sawlog-sized spruce stems, root rot causes decay at the stem base, while healthy sawlogs can be obtained from higher up along the stem. In this work, we assume that the root rot indicated by the algorithm is caused by *H. parviporum*. Details of the rot detection algorithm are given in Appendix I.

2.3. Splitting the stand into infected and healthy microstands

2.3.1. Purely spatial approach using DBSCAN

From the harvester data, the position of each stump can be approximately obtained by estimating the position of the harvester head at the time of performing the felling cut for the stem. This estimation is done in this work by using the GNSS-measured position of the harvester cabin, the orientation of the front axle and the boom, and the boom length (Taipale et al. 2022). By pairing the rot status of each spruce stump as obtained from the rot algorithm (Section 2.2) with the location of each stump, we obtain a map of the freshly felled stand which shows the rot status of each spruce tree. For spruce stems whose dimensions do not fulfill the requirements for a sawlog stem, the rot algorithm always returns "false" for the rot status. The rot status of these smaller stems must therefore be considered unknown in the tree map. The task is then to find the infected regions of the stand, i.e., those regions where the next generation of spruce would become infected by *H. parviporum*. The regions outside of the infected regions are considered healthy, i.e., these are regions where spruce can grow free of root rot disease.

In the purely spatial approach, we consider solely the spruce stems for which the algorithm reported a positive rot detection result. To derive the infected regions of the stand, we apply the scikit-learn implementation (Pedregosa et al. 2011) of the non-parametric clustering method DBSCAN to the positions of the stumps of the rotten stems in the horizontal plane. DBSCAN is controlled by two parameters: ε and $n_{samples}^{min}$, which together determine the size of the created clusters for a given set of points. Points outside of the clusters are labeled as outliers. Our interpretation is that clusters describe "hotspots" of root rot, or disease centers, whereas the outliers describe individual, isolated rotten spruce stems.

After applying DBSCAN to the stump data, we delineate the infected areas using alpha shapes as implemented by Bellock (2024). Considering each rot cluster at a time, we find the optimal alpha parameter (Bellock 2024) and then perform the delineation using this value. We set an extra buffer of 10 m for the infected delineations to make areas outside of these delineations reasonably safe for planting a new generation of spruce. The value of 10 m was arrived at through considering the mean error of 4 m between the recorded and true position of the stumps (Taipale et al. 2022) and additionally that several meters are required between the stump of a rotten spruce tree and newly planted spruce to avoid infection in the new tree (Piri 2003). For each of the rotten outlier stems, we simply create a circular delineation of 10 m in radius centered at the stump.

Next, we delineate the entire stand, i.e., harvest area, using all the harvested stems of all species. We then take the union of the infected area delineations, and then the intersection of the entire stand delineation polygon with this union to find the total infected region. Finally, we take the difference of the entire stand delineation polygon and the total infected region to find the total healthy region of the stand. The total infected and the total healthy region constitute the splitting of the stand into microstands. The entire process is illustrated with an example stand in Fig. 2.

2.3.2. Probabilistic approach using Bayesian modeling

As an alternative to the purely spatial approach (Section 2.3.1), we delineate the infected and healthy microstands using a probabilistic algorithm. The algorithm has three major steps. First, a parametric infection kernel, modeling the infection spread via root systems, is estimated from the known-status, i.e., sawlog-sized spruce stems using a purpose-built Bayesian hierarchical model. Second, using the calibrated model and its estimate of the distribution of infected spruce trees in the generation prior to the one just felled, we compute the (past) probability of infection for any unknown-status spruces in the stand, and then generate 500 stochastically imputed, pseudo-complete known-status spruce stem datasets. Third, we apply the calibrated parametric infection kernel to each imputed dataset to create 500 (future) risk maps, which are then pooled to create a probabilistic infection risk map for the stand. The probabilistic infection risk map is finally binarized into healthy/infected regions using the rule $P(risk \leq 10\%) \geq 95\%$, i.e., we want to be highly certain ($\geq 95\%$) that the infection risk for new spruce trees is very low ($\leq 10\%$) in the healthy microstand. The entire process is illustrated with an example stand in Fig. 3. Further details on the algorithm are provided in Appendix II.

2.4. The regeneration alternatives

The goal of our method is to provide the forest owner decision support when regenerating their stand after clearcutting so that root rot is eradicated from the stand, and subject to this condition, either the financial result or climate change mitigation value of the stand is maximized. To produce the regeneration recommendations to achieve this, we consider a fixed set of 10 different alternative regeneration plans and find the best one of these, individually maximizing either BLV or net CO_2 removals by living tree biomass (Section 2.1, Fig. 1). We assume that *H. parviporum* is the only pathogen present at the site.

We consider four different choices of tree species in constructing the regeneration alternatives: spruce, birch, pine, and a 50%-50% mixture of spruce and birch. The first four regeneration plans (alternatives 1 to 4 below) involve planting the entire stand with a single tree species. These alternatives were chosen for their simplicity and because they serve as useful references for the other alternatives and for the microstand approach itself. Then, we consider three cases of cleansing the infected areas by planting pine into these areas, and planting, in turn, each of the three remaining choices of species outside of the diseased areas (alternatives 5 to 7). Finally, we consider three cases of cleansing the infected areas by using birch in these areas and planting each of the three remaining choices of species elsewhere (alternatives 8 to 10). In total, the 10 regeneration alternatives that we consider are the following:

1. Spruce for the entire stand
2. Spruce-birch mixture for the entire stand
3. Birch for the entire stand
4. Pine for the entire stand
5. Pine for the infected areas, spruce elsewhere
6. Pine for the infected areas, spruce-birch mixture elsewhere
7. Pine for the infected areas, birch elsewhere
8. Birch for the infected areas, spruce elsewhere
9. Birch for the infected areas, spruce-birch mixture elsewhere
10. Birch for the infected areas, pine elsewhere

2.5. Simulations of forest growth and Heterobasidion dynamics

2.5.1. Forest growth on healthy sites: Motti simulations

Stand projections for healthy sites were generated with the Motti stand simulator (henceforth Motti). Motti is a stand-level decision-support tool for assessing the effects of forest management on stand dynamics (e.g., Hynynen et al. 2015, Juutinen et al. 2018). Motti consists of stand-level and individual-tree level distant-independent models. Both the stand-level and individual-tree level models are based on an empirical-statistical modeling approach with an extensive body of long-term growth and yield data from managed forests covering Finland (Matala et al. 2003, Hynynen et al. 2014). Stand-level models are applied for natural regeneration and early growth, while individual-tree level models are used to predict growth for mature trees, i.e., trees with dominant height > ca. 7 m. Motti is a software package that produces stand projections for management options based on repeated thinnings from below and clearcutting, i.e., rotation forestry (Matala et al. 2003, Hynynen et al. 2014). Earlier results indicate that Motti is generally a reliable tool for comparing forest management alternatives in Finnish conditions (e.g., Mönkkönen et al. 2014, Juutinen et al. 2018).

Thus far Motti has been widely applied both at stand level (e.g., Hynynen et al. 2005, Haapanen et al. 2016, Ahtikoski and Hökkä 2019) and in landscape-level analyses (e.g., Mönkkönen et al. 2014, Hynynen et al. 2015, Ahtikoski et al. 2024). In this study, Motti was used to produce stand projections according to silvicultural guidelines (Äijälä et al. 2019) specifically set for different tree species (spruce, pine, and birch), site types (mesic heath (MT), herb-rich heath (OMT)) and for a mixture of spruce and birch. These silvicultural guidelines are based on socially, environmentally, and economically sustainable forest management. The silvicultural guidelines determine the timing and intensity of thinnings so that specific basal area limits to conduct a thinning are set as a function of dominant height, and the timing for a clearcut is determined either by mean tree diameter or stand age (Äijälä et al. 2019). The stand projections here were produced for 15 different temperature sums in the range of approximately 1050 to 1350 degree days °C (d.d.) with a 5 °C threshold.

Motti also includes empirical biomass models by Repola (2008, 2009), which provide tree level estimates for biomass by components (stem, branches, leaves, stump, and woody roots). These biomass estimates were used to estimate carbon stock dynamics of growing stands by assuming that 0.5 (the precise value varying slightly by biomass component) of the living tree biomass is carbon. The thus estimated carbon mass was then converted into CO_2 mass by multiplying by 44/12. The resulting CO_2 mass (in units of tCO_2) describes the net CO_2 removals by the living tree biomass at a given point in time in the rotation period. The obtained CO_2 mass can also be taken to represent the living biomass carbon stock of the stand through the mass of CO_2 that would result from turning the carbon present in the biomass into CO_2.

In assessing the BLV (based on stand projections of healthy sites), stumpage prices and per unit silvicultural costs were derived from a time series covering the years 2011–2020. At the time of our analyses, this series was the most recent 10-year period available. Then, nominal prices and costs were further converted to real prices through deflation (applying the cost-of-living index of Statistics Finland 2020, http://www.stat.fi/til/khi/index_en.html). The rationale of using a 10-year time series was to include peak and bottom prices and costs into the calculation of the average to capture the effect of variation in real terms (see Ahtikoski et al. 2024 for absolute values of prices and costs identical to those used in this study). When computing the BLV, all silvicultural costs except the cost of removing naturally regenerated spruce saplings from the stand after changing the tree species from spruce to birch or pine were taken into account. An interest rate of 2% was used in all BLV calculations throughout this work.

2.5.2. Forest growth on infected sites: Motti+Hmodel simulations

Stand projections with Heterobasidion root rot were simulated using

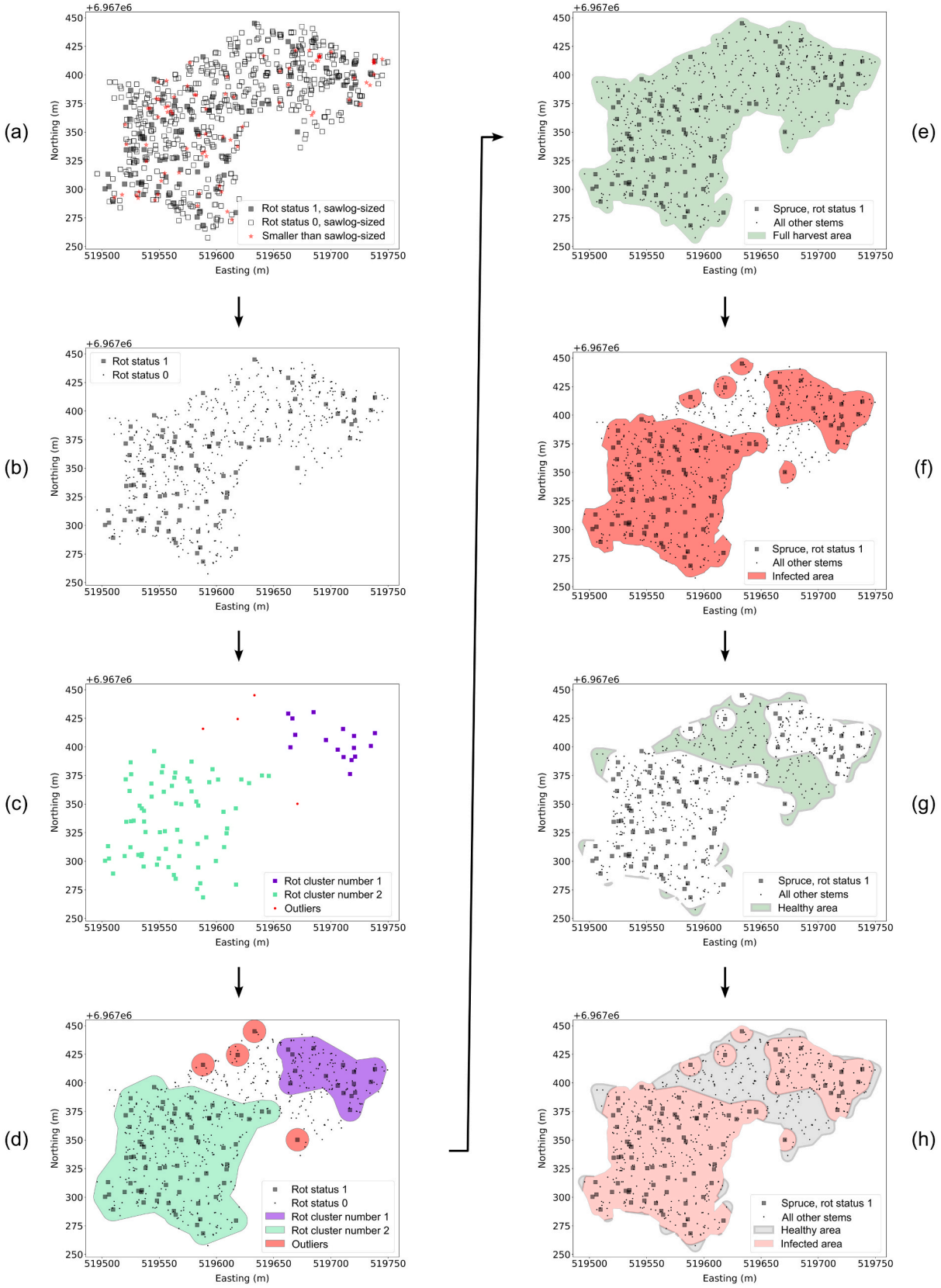

Fig. 2. Splitting a forest stand into healthy and infected microstands using the purely spatial approach (DBSCAN). (a) The result of applying the stem-level rot detection algorithm to the harvester data (Section 2.2). (b) Only the spruce stems with a positive rot status are used in finding the infected microstands. (c) Applying DBSCAN to the spruce stems with positive rot status. (d) Delineating each DBSCAN cluster using a buffered alpha shape and placing a circular delineation at each outlier stem. (e) Delineating the entire harvest area using all stems. (f) Taking the union of the infected delineations and then the intersection of this union with the entire harvest area delineation to find the total infected region of the stand. (g) Taking the difference between the entire harvest area delineation and the total infected region to find the total healthy region of the stand. (h) The final microstand setup for this stand, i.e., the total healthy region and the total infected region.

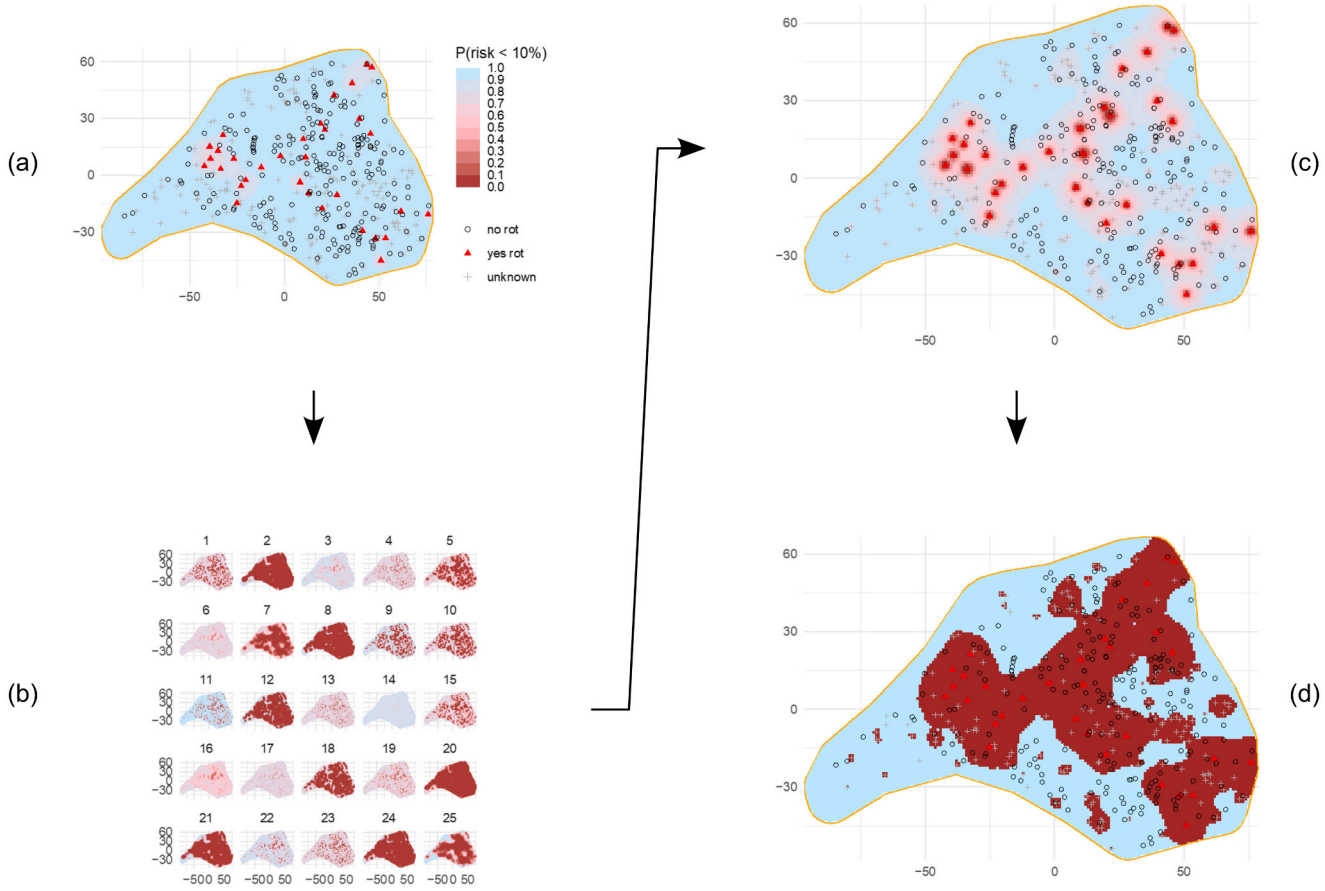

Fig. 3. Splitting a forest stand into healthy and infected microstands using the probabilistic approach. The coordinates are given with respect to the center of the stand (mean position of stems) in units of m. (a) By estimating a parametric infection kernel and the distribution of infected trees in the generation prior to the one just felled, a map of past infection risk is created for the stand. (b) Using the map of past risk, the rot status is stochastically imputed for stems for which the status unknown, i.e., smaller than sawlog-sized stems. (c) Using the calibrated infection kernel and the imputed and known rot values for the stems, a map of future infection risk is created. (d) Finally, the future risk map is binarized into healthy and infected microstands.

the Motti stand simulator integrated with Hmodel, which simulates the disease dynamics in time and space (Honkaniemi et al., 2014, 2017). Hmodel is a spatially explicit extension to Motti that creates locations for each stump and tree in the stand and simulates the Heterobasidion root rot spatial spread and growth within trees, finally affecting tree growth and yield simulated by Motti as described above (Section 2.5.1). In Hmodel, the key processes of *Heterobasidion* spp. are simulated with an annual time step starting from the initialization of a stand until the final felling and taking all the forest management operations in adherence to the national silvicultural guidelines into account. Hmodel has been developed and validated by the principles of Pattern-Oriented Modeling (Grimm and Railsback, 2012; Honkaniemi et al., 2014, 2017).

We used Hmodel to simulate the development of Norway spruce stands and mixed spruce-birch stands in three different temperature sum regions (1100, 1250, and 1300 d.d.) at two different site types (MT, OMT). Due to stochasticity in the model structure related especially to the explicit locations of trees, each simulation was repeated 10 times. We assumed that the only causal agent of root rot disease was *H. parviporum* specialized in Norway spruce, and thus change of tree species would result in eradication of the disease over time. *Heterobasidion* dynamics were simulated assuming that the primary infections occurred only at the stand initialization ($t = 0$) with varying spore pressure, and secondary infections were initiated from previous tree generation stumps with varying levels of disease (0%, 10%, 30% or 60% of spruce trees of the previous generation being infected). From these infections, the disease spreads to the living tree generation and causes growth losses, mortality, and reduction of timber quality. The quality reductions affect timber assortments during harvests and thus result in economic losses compared to the abovementioned healthy stands. When computing the BLV, all silvicultural costs were taken into account.

2.5.3. *Generalizing the simulation results to arbitrary temperature sum and rot status of the previous tree generation*

The results of the Motti (Section 2.5.1) and Motti+Hmodel (Section 2.5.2) simulations for BLV and maximum net CO_2 removals are visualized in Fig. 4. Due to differences in growth models, a corrective scaling was required to align the Motti+Hmodel results (Section 2.5.2) with the Motti results for healthy stands (Section 2.5.1). This was done by multiplying, at each temperature sum, the four BLV results for infected spruce or spruce-birch stands by the ratio of the Motti result and the Motti+Hmodel result for the healthy stand (0% of the previous spruce generation being infected), and similarly for the CO_2 results.

The data in Fig. 4 are used in the regeneration optimization to estimate the BLV and CO_2 result for each considered regeneration alternative (Section 2.4). For this purpose, the simulation results of Fig. 4 needed to be generalized to produce the BLV and maximum attainable net CO_2 removals (C) for any of the four tree species selections, per ha, at any desired temperature sum (T_{sum}) and fraction of rotten spruce trees in the previous generation (rot fraction, f_{rot}). To achieve this, for each site type considered in this work (MT, OMT), we smoothed the simulation data for each species selection to produce functions for the BLV and CO_2 results with T_{sum} and f_{rot} as the independent variables. More formally, we produced the functions

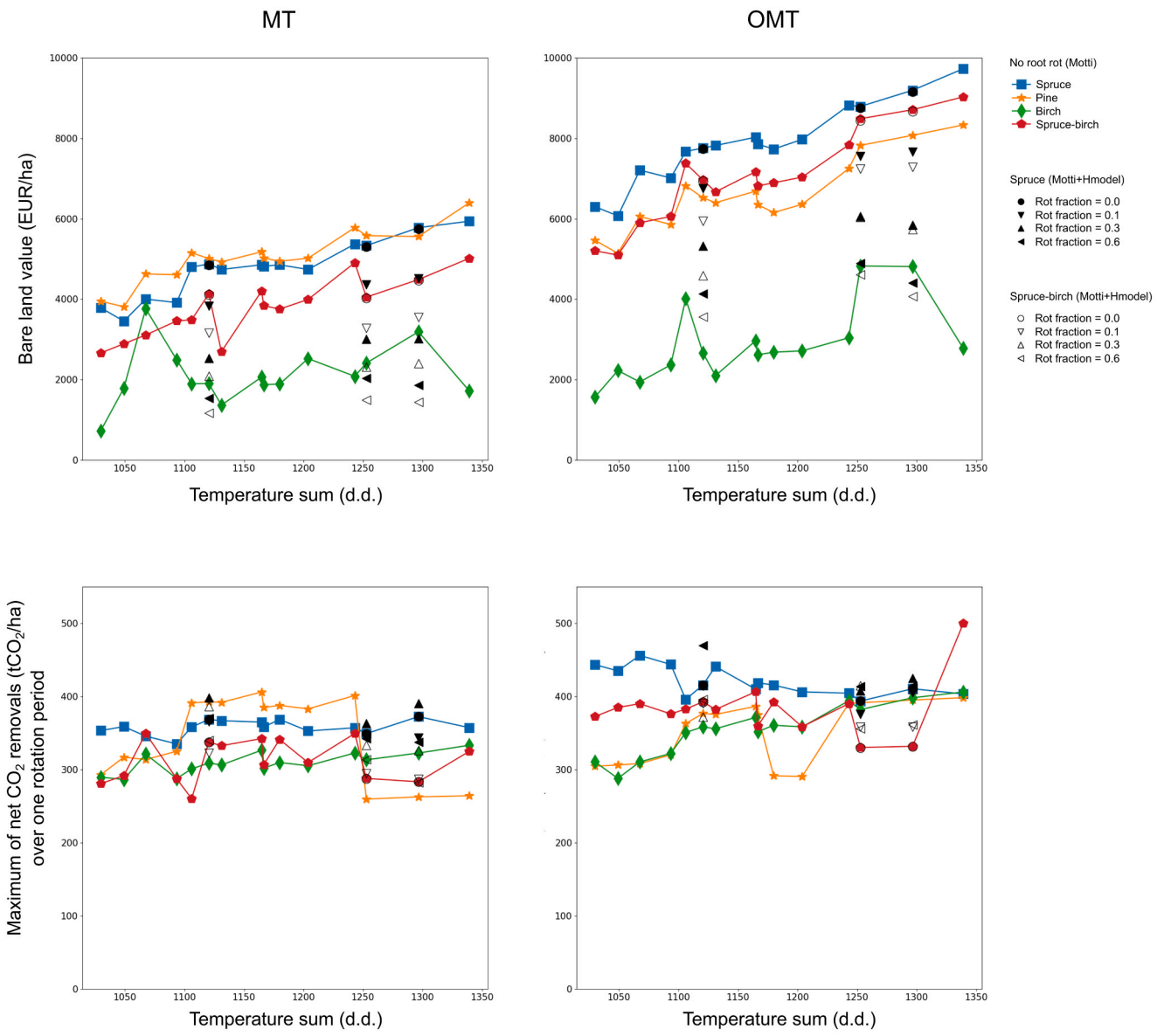

Fig. 4. Results from the Motti and Motti+Hmodel simulations for BLV (upper row) and maximum net CO_2 removals (bottom row) for each tree species on each site type (mesic heath (MT), herb-rich heath (OMT)). Each point in the presented Motti+Hmodel results is an average over four different spore pressures and 10 random initializations for each spore pressure, i.e., 40 individual simulations. Rot fraction is the fraction of spruce trees of the previous generation that were infected by *H. parviporum*. The interest rate for the BLV results is 2%.

$$BLV = BLV_j^i(T_{sum}, f_{rot}) \tag{1}$$

$$C = C_j^i(T_{sum}, f_{rot}) \tag{2}$$

where $i \in \{\text{birch, pine, spruce, spruce-birch mixture}\}$ and $j \in \{\text{MT, OMT}\}$.

To do the smoothing, we used LOESS as implemented by Cappellari et al. (2013). For birch and pine, the BLV and CO_2 results are independent of the infection status of the previous tree generation. Therefore, for these species, we performed LOESS in one dimension to find $BLV = BLV_j^i(T_{sum})$ and $C = C_j^i(T_{sum})$. For spruce and the spruce-birch mixture, we performed LOESS in two dimensions to find $BLV_j^i(T_{sum}, f_{rot})$ and $C_j^i(T_{sum}, f_{rot})$. In the local regression, we used a first-degree polynomial for the one-dimensional case, and a first-degree bivariate polynomial, i.e., a plane, for the two-dimensional case.

The LOESS smoothing is controlled by the size of the local neighborhood (N_{local}), i.e., the number of the nearest points to x used to perform the local regression at x. To find the optimal choice of N_{local}, we considered the values $N_{local} = 5, 10, 15$ for the univariate case and $N_{local} = 10, 15, 24$ for the bivariate case, here the number of points in the full simulation data being 15 for the former and 24 for the latter. By visually assessing the resulting smoothings against the simulation data, we chose $N_{local} = 10$ for the univariate case and $N_{local} = 24$ for the bivariate case. We produced the smoothing at intervals of 1 d.d. for T_{sum} and 0.01 for f_{rot}. Visualizations of the final functions for both the BLV and CO_2 results are given in Appendix III.

2.6. Computing the BLV and the maximum of net CO_2 removals for each regeneration alternative

To find the optimal regeneration plan out of the 10 alternatives for the stand (Section 2.4), we use the regression functions of Section 2.5.3 to estimate the BLV and CO_2 result for each alternative. This is done as follows.

The total BLV of the stand, for a given regeneration plan, is computed

as the sum of the BLVs of the individual microstands. The calculation is done using the per ha values of the BLV of the different tree species and the areas of the microstands:

$$BLV = \sum_{i=1}^{N_{microstands}} BLV_d^{s_i}(T_{sum}, f_{rot}^i) \bullet A_i \quad (3)$$

where $N_{microstands}$ is the number of microstands, $BLV_d^{s_i}$ is the function of Eq. (1) in units of EUR/ha, d is the site type, i.e., the most frequent fertility class under the stems of the stand (Section 2.7), s_i is the species planted into microstand i, and A_i is the area of the microstand in ha. Here microstand can mean either the entire stand, the total healthy region, or the total infected region. The fraction of rotten sawlog spruce stems in the previous generation (f_{rot}^i) is computed from the harvester data for the microstand in question. The temperature sum (T_{sum}) is obtained from a pre-computed database of the mean annual temperature sum in the period 1971 to 2000 formed using the methodology of Ojansuu and Henttonen (1983). The set of pre-computed temperature sums is visualized in Appendix IV. The temperature sum of the stand being processed is set to the temperature sum of the geographically closest point (by Euclidean distance) in the pre-computed data.

We assume that $f_{rot} = 0$ outside of the infected areas, and that stump treatment during the management of the stand (i.e., thinnings) is done sufficiently well to prevent new *Heterobasidion* infections from appearing into the healthy area. This approach to computing the BLV of the stand corresponds to permanent establishment of the stand using the given regeneration plan for an infinite number of rotation periods. The calculation of the total BLV for the stand is illustrated in Fig. 5 for two examples of regeneration plans.

When computing the BLV (or CO_2) result for spruce or spruce-birch using the Hmodel results, a small discrepancy is introduced due to the previous generation of trees in the Hmodel simulations being almost purely spruce, whereas when computing the BLV (or CO_2) result for alternatives 1 and 2 (Section 2.4) using our method, the previous generation of trees of the actual harvested stand may have included other trees besides spruce. Our method can therefore be considered more accurate the closer the felled stand being regenerated was to a pure spruce stand.

Computing the maximum net CO_2 removals for a given regeneration plan is done completely analogously to the BLV calculation (Eq. (3)). The only difference is that instead of a BLV function, we use the relevant CO_2 function (giving the maximum attainable net CO_2 removals per ha):

$$C = \sum_{i=1}^{N_{microstands}} C_d^{s_i}(T_{sum}, f_{rot}^i) \bullet A_i \quad (4)$$

This approach to computing the net CO_2 removals by the stand living tree biomass produces, in practice, an estimate for the value to which the total net CO_2 removals by the stand saturate towards the end of the rotation period using the given regeneration plan. This is because for each tree species, the net CO_2 removals per ha, or equivalently, the living tree biomass carbon stock as expressed in tCO_2/ha, saturates to its maximum value towards the end of the rotation period.

2.7. Assessing the optimization method on a validation dataset of stands

To study the distribution of recommendations that our optimization method produces for real forest stands, to estimate the potential benefits of using our method, and to find out whether purely economically optimal regeneration eradicates root rot from infected stands, we applied the method to a set of 269 clear-cut stands with varying degrees of root rot in the previous generation of spruce trees. The stands were selected based on the following criteria from a much larger set of mainly spruce-dominated stands from Southern and Central Finland.

First, as our BLV and CO_2 models are only applicable on mineral soils, it was required that most of the stems in each stand are located on mineral soil according to the Finnish Forest Centre open soil type data (Finnish Forest Centre 2024). Second, the most frequent site type (i.e., fertility class) under the stems of each stand was required to be either OMT or MT, according to the Finnish Forest Centre open fertility class data (Finnish Forest Centre 2024). Third, stands with less than 100 stems and stands containing no rotten sawlog-sized spruce stems were discarded. The resulting 269 stands were harvested between January 2019 and December 2021. Distributions of the key stand-level properties for the stands at the time of harvesting are given in Fig. 6. In the following, we refer to this set of stands as our validation set.

As described in Section 2.3, we considered two different approaches to splitting a stand into the healthy and infected regions. The DBSCAN-based approach is controlled by the parameters ε and $n_{samples}^{min}$, which can be tuned to perform delineations from extremely fragmented (i.e., each rotten spruce stem constituting its own circular delineation) to broader and smoother delineations (i.e., a low amount of large rot clusters). Moreover, in the Bayes approach, the imputing of rot values for the unknown cases, i.e., below sawlog-sized harvested stems, can be switched on or off when producing the infected area delineations. As the BLV and CO_2 results for a regeneration plan can be expected to vary depending on the areas of the delineations, we processed the full set of 269 stands using five different delineation approaches. There were three varieties of the purely spatial approach: "DBSCAN, fragmented" ($\varepsilon = 0.001$ and $n_{samples}^{min} = 999$), which considered each rotten spruce stem as an individual outlier, "DBSCAN, average" ($\varepsilon = 30$ and $n_{samples}^{min} = 4$), which produced fairly large clusters of rotten stems and some outliers, and "DBSCAN, broad" ($\varepsilon = 40$ and $n_{samples}^{min} = 3$) which produced

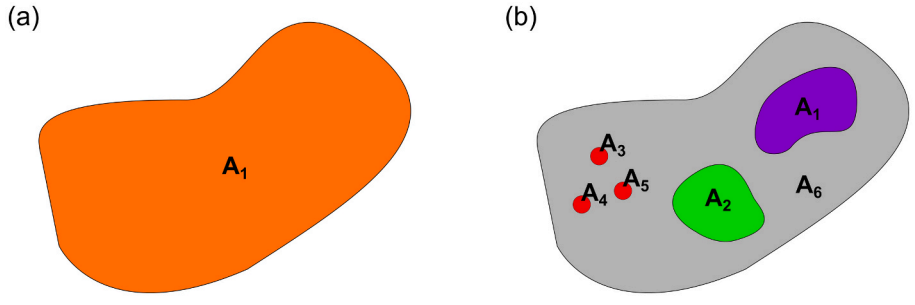

Fig. 5. Schematic example of a stand and computing the BLV for two of the 10 alternative regeneration plans (Section 2.4). (a) Alternative no. 2: planting a spruce-birch mixture for the entire stand. In this plan, the stand consists of a single "microstand" which is the stand itself. The area of the single microstand is A_1. The overall rot fraction f_{rot} of the stand is used in computing the BLV via Eq. (3). (b) Alternative no. 5: planting pine into the infected areas and spruce elsewhere. Here the stand consists of two microstands. The first microstand is the total infected region, which is the union of the violet, green, and red delineations with areas A1, A2 and A3, A4 and A5, respectively. The second microstand is the total healthy region, i.e., the grey region, which has an area of A6. In the infected microstand, the BLV contribution is independent of f_{rot}, because the BLV result for pine does not depend on f_{rot}. In the healthy microstand, we assume $f_{rot} = 0$ when computing the BLV contribution that comes from spruce.

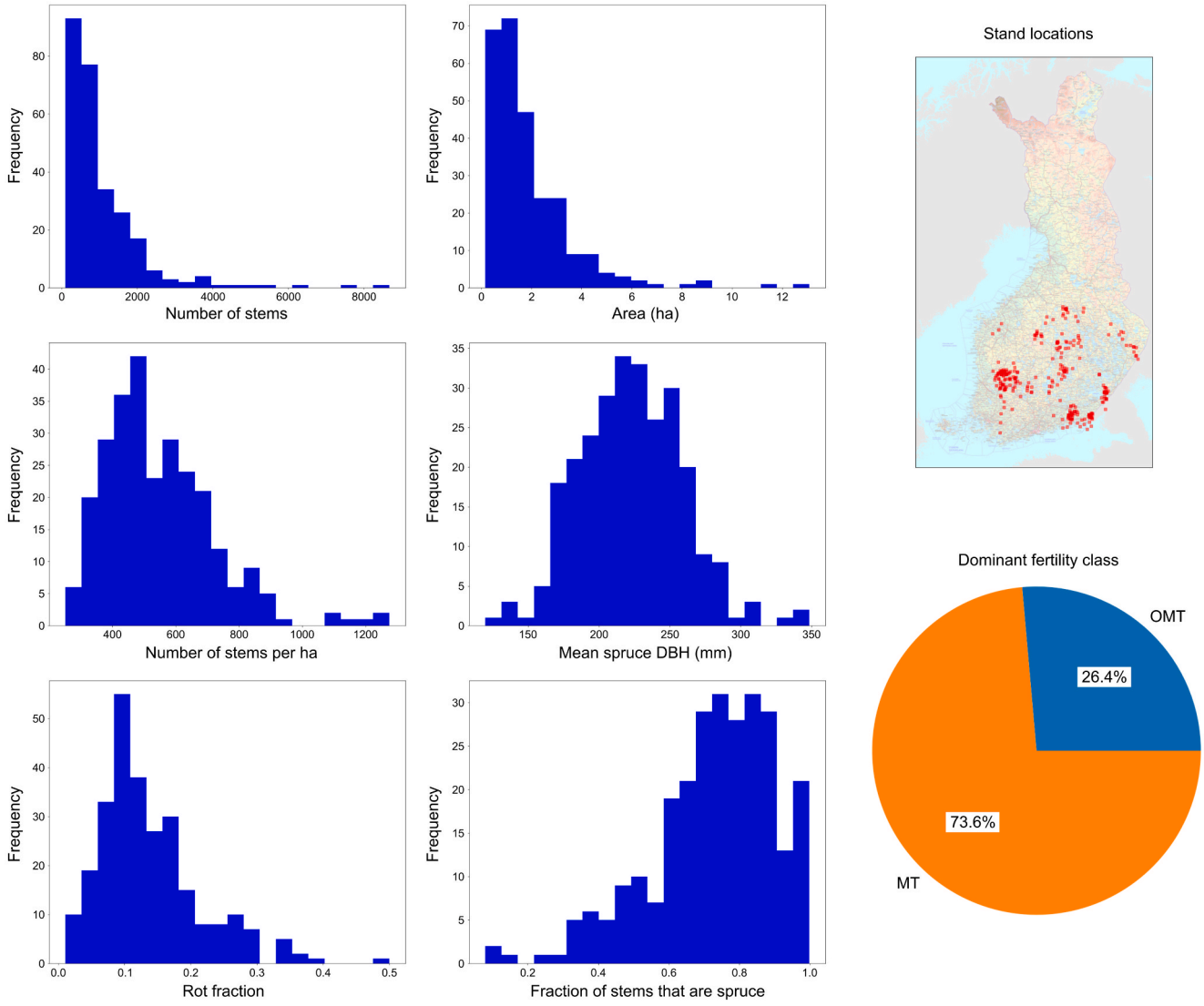

Fig. 6. Distributions of key properties and the positions of the stands of our validation set of 269 clear-cut stands in Finland. The background raster map of Finland is distributed by the National Land Survey of Finland under the CC BY 4.0 license.

even larger rot clusters. In addition, we considered the Bayes approach with or without imputing for the unknown rot states of stumps. For each delineation approach, the optimized solutions, i.e., regeneration recommendations, were determined for each of the 269 stands. In addition, the gain in BLV or net CO_2 removals per ha was computed for each stand with respect to regenerating the stand with only spruce, as well as with respect to regenerating the stand with the best single-species alternative that purifies the stand.

3. Results

In this section, we present the results of applying our optimization method on the validation set of 269 recently clear-cut stands in Finland (Section 2.7). In Section 3.1, we give examples of microstand delineations, i.e., splitting of the stands into healthy and infected regions. In Section 3.2, we present the distributions of the regeneration plans in terms of tree species selection. In Section 3.3, we present the benefits of the optimization in terms of financial and carbon results. In Section 3.4, we assess the financial cost of eradicating root rot using our method.

3.1. Microstand delineations

Examples of the results of splitting stands into the healthy and infected delineations using the five different approaches on the validation set, i.e., three DBSCAN approaches and two Bayes approaches (Section 2.7), are shown in Fig. 7. As can be seen by comparing these examples, the Bayes approach typically produces smaller infected areas than the DBSCAN approach does. Delineations produced using DBSCAN also appear smoother, even for the extreme case of "DBSCAN, fragmented."

A key difference between the Bayes and DBSCAN approaches is that the DBSCAN approach operates solely on stumps with known positive rot status, whereas in the Bayes approach, the unknown values, which are associated with all smaller than sawlog-sized spruce stumps, can also be taken into account. As can be expected, this sometimes leads to situations where for a given stand, the Bayes approach identifies as infected regions within the stand that the DBSCAN approach, even with the "DBSCAN, broad" variant, delineates into the healthy region. Examples of this are shown in Fig. 8.

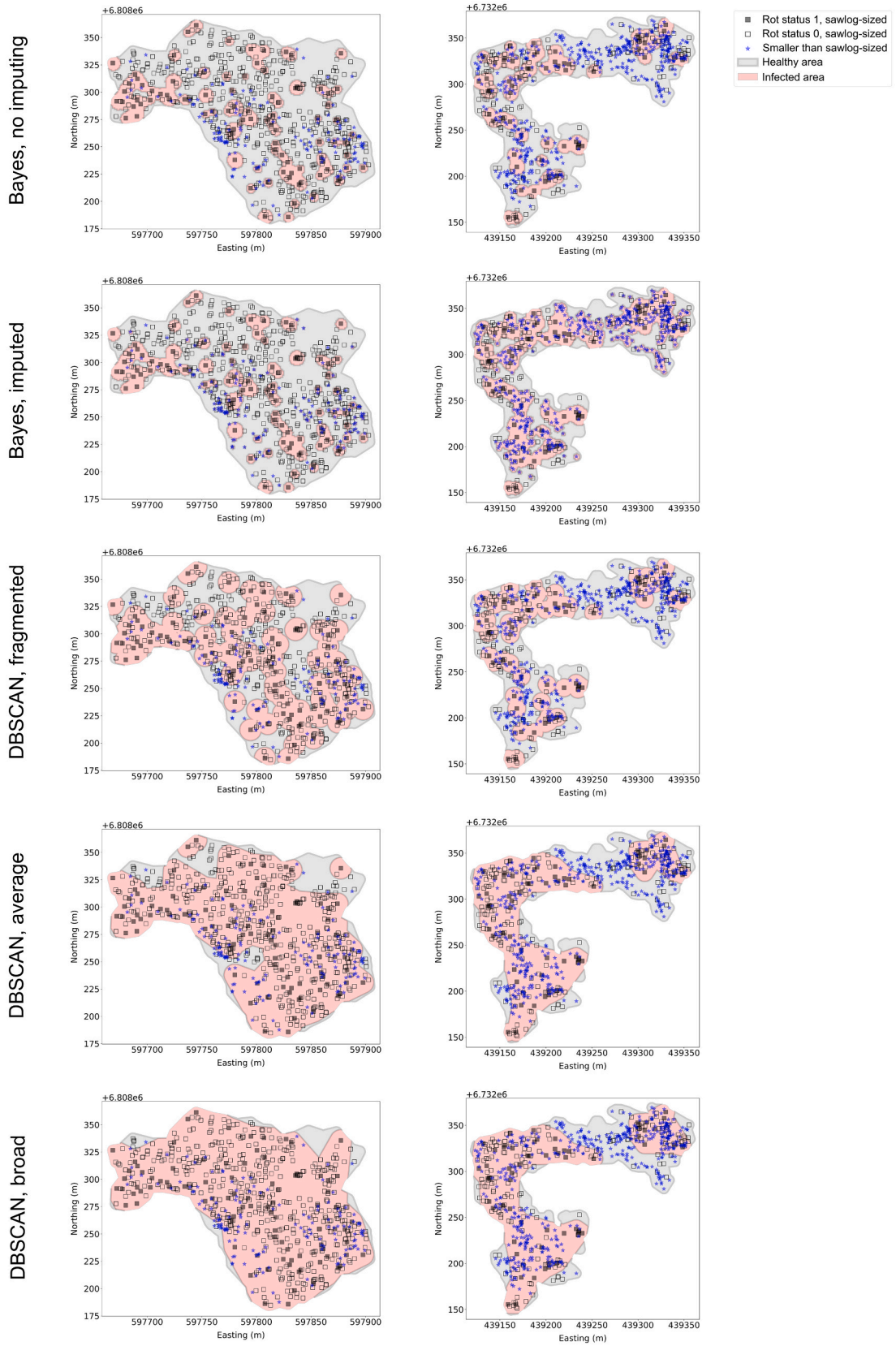

Fig. 7. The final delineation into healthy and infected regions for two example stands, for all the five considered delineation approaches.

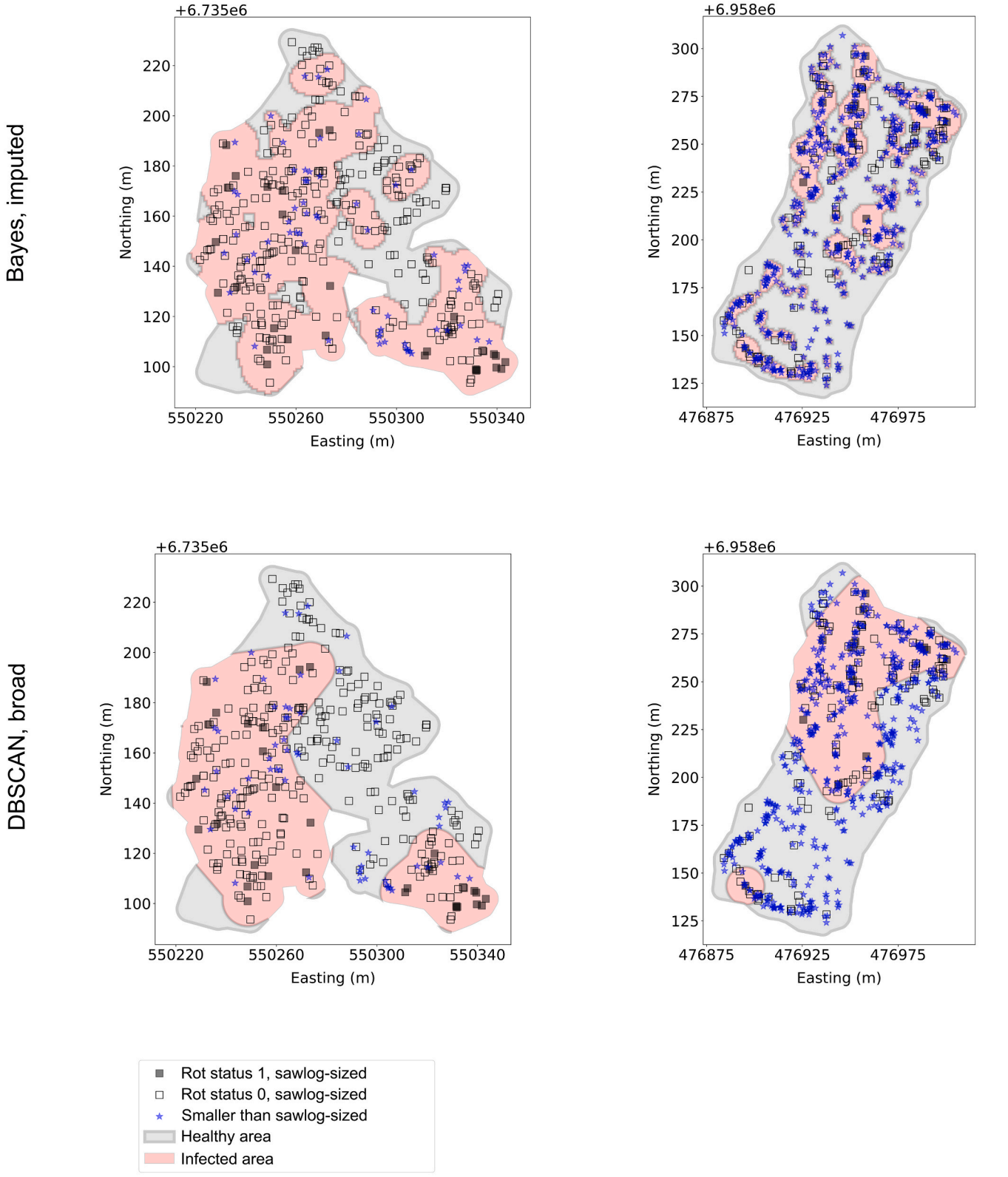

Fig. 8. Since the DBSCAN delineation approaches are based purely on the spatial configuration of known rotten stumps of sawlog-sized spruce trees, they do not take into account the unknown status of smaller-than sawlog-sized spruce trees. The Bayes approach, on the other hand, can take these unknown values into account through imputing values for the unknown rot states of stumps. This can lead to predictions for new infected areas that the DBSCAN approach does not capture, as shown for two example stands here.

3.2. Optimal choice of tree species

When applying our optimization method to the validation set (Section 2.7), we find that when optimizing for BLV, the recommended tree species on MT type sites is practically always pine for the entire stand. On OMT sites, the solution is universally to plant pine for the infected areas and spruce outside of the infected areas. When optimizing for net CO_2 removals, the solutions on both site types are more diverse and they often include birch. The recommendations for optimizing CO_2 removals vary with the temperature sum of the stand. A more detailed analysis is presented in the following two sections.

3.2.1. Free optimization

We present the distribution of the optimal regeneration plans over the validation set in terms of tree species selection in Fig. 9, separately for MT and OMT sites. In addition to showing the results for the optimization subject to the condition that the stand is purified of root rot, which constitute the ultimate recommendations produced by our method, we present the corresponding results also for the case of "free optimization," where cleansing of the stand is not required. The optimal regeneration plan in this free optimization is simply that, out of the 10 considered alternatives, which maximizes the BLV or CO_2 result. The results in Fig. 9 are shown for the "DBSCAN, average" delineation approach, because for all cases except BLV maximization in free optimization on OMT, the distribution of the optimal choice of tree species

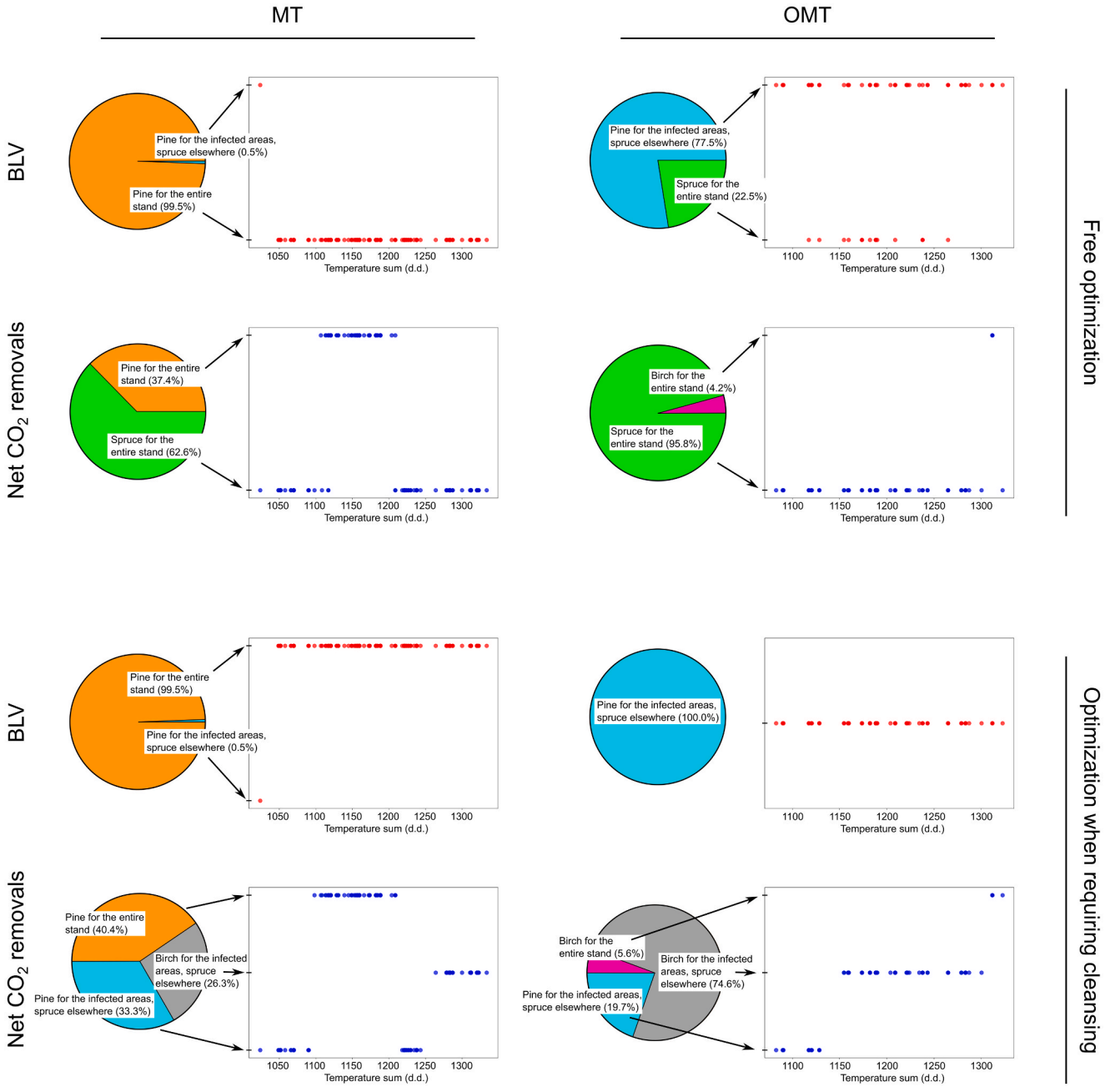

Fig. 9. Distributions of the optimal choice of tree species for the two considered site types (mesic heath (MT), herb-rich heath (OMT)) and the two separate optimization metrics (BLV, net CO_2 removals) for the "DBSCAN, average" delineation approach on the validation set. The results are presented for "free optimization," where the metric in question is maximized with no constraints (upper panel) and for optimization subject to the condition that the stand becomes purified of root rot disease (lower panel).

and the behavior of the optimal choice of tree species as a function of temperature sum are independent of the delineation method.

First, considering the case of free optimization, when maximizing BLV, the recommended tree species choice on practically all MT sites is "pine for the entire stand" (Fig. 9). This result clearly reflects the simulation data underlying the optimization (Fig. 4), where it is evident that pine provides the highest EUR/ha, regardless of rot fraction, for virtually the entire range of temperature sums. The situation is different on OMT sites. The regeneration plan "pine for the infected areas, spruce elsewhere" makes up the majority of the optimized plans (77.5% of cases). In the remaining 22.5% of cases, the strongest option is "spruce for the entire stand." By examining the simulation data of Fig. 4 and the list of possible regeneration alternatives, one could indeed expect that these two options dominate the free optimization results.

Since at any given temperature sum on OMT sites, the spruce result for EUR/ha crosses the pine result as the rot fraction is increased (Fig. 4), it follows that the rot fraction of the stand, as well as the size of the total infected area relative to the stand area, determine which of the two options, "spruce for the entire stand" or "pine for the infected areas, spruce outside of rot areas" gives the highest total BLV for the stand. By choosing "pine for the infected areas, spruce elsewhere," the overall EUR/ha of the solution will settle somewhere between that of pure pine and healthy spruce. The overall EUR/ha varies linearly as a function of the ratio of the infected area to the full stand area. If this ratio is close to zero, then the EUR/ha will be close to that of healthy spruce. If the ratio is close to one, then the EUR/ha will be close to that of pure pine.

Therefore, when the rot fraction is high enough that the spruce EUR/ha is below the pine function, the best solution of the two is always "pine for the infected areas, spruce elsewhere." But when the rot fraction is low enough that the spruce BLV function is between those of pine and healthy spruce, then the rot fraction and the ratio of the infected area to the full stand area determine whether it is better to stay with "spruce for the entire stand" or to use "pine for the infected areas, spruce elsewhere." In the OMT stands of our validation set, for each delineation method, the average rot fraction is lower for stands where the best option is "all-spruce" when compared to stands where the best option is "pine for the infected areas, spruce elsewhere." When comparing results between the different delineation approaches, the larger the share of infected area, the more cases appear where "all spruce" is the best solution (Table 1).

When maximizing the net CO_2 removals by the stand, "spruce for the entire stand" is the dominating solution on both MT and OMT sites, being the optimal solution for 62.6% and 95.8% of stands, respectively (Fig. 9). On MT sites, the other realized solution is "pine for the entire stand," whereas for OMT it is "birch for the entire stand." These results, along with the dependence of the optimal solution on temperature sum, again clearly reflect the simulation results (Fig. 4).

3.2.2. Optimization when requiring eradication of root rot

When performing the BLV optimization subject to the requirement that the stand is cleansed of root rot disease, the optimal tree species selection for MT sites is nearly always "pine for the entire stand" (Fig. 9). On OMT sites, the recommendation is now "pine for the infected areas, spruce elsewhere" for all stands. However, when maximizing net CO_2 removals of the stand, the results are more diverse. Depending on the temperature sum, the optimal solution on MT sites varies between "pine for the infected areas, spruce elsewhere," "pine for the entire stand," and "birch for the infected areas, spruce elsewhere." On OMT sites, the optimal solution in terms of tree species is "pine for the infected areas, spruce elsewhere," "birch for the infected areas, spruce elsewhere," and "birch for the entire stand," depending on the temperature sum. These results and the choice of optimal species as a function of temperature sum again clearly reflect the underlying simulation data (Fig. 4).

Table 1
The percentage of "spruce for the entire stand" in the set of optimal solutions when doing "free optimization" of BLV on OMT sites of the validation set, given separately for each delineation approach. The complement fraction of the solutions is "pine for the infected areas, spruce elsewhere" in all cases of OMT. The mean of the share of the total infected area out of the total stand area is given also. The error is the standard error of the mean.

	Bayes, no imputing	Bayes, with imputing	DBSCAN, fragmented	DBSCAN, average	DBSCAN, broad
Percentage of "spruce for the entire stand" in the optimal solutions (OMT sites)	0.0	1.4	4.2	22.5	31.0
Ratio of infected area to total stand area (OMT sites)	0.34 +- 0.02	0.41 +- 0.03	0.53 +- 0.02	0.64 +- 0.03	0.69 +- 0.03
Ratio of infected area to total stand area (MT and OMT sites pooled)	0.307 +- 0.012	0.373 +- 0.013	0.502 +- 0.012	0.621 +- 0.015	0.679 +- 0.014

3.3. Benefits of the optimization in terms of the BLV and CO_2 removals

3.3.1. Benefits with respect to regenerating with spruce only

The benefits of performing the optimization, with respect to regenerating each stand using only spruce, are given in Fig. 10 as histograms and as a function of temperature sum for "DBSCAN, average." When maximizing BLV and requiring eradication of root rot, we find the mean gain in BLV on MT sites of the validation set (Section 2.7) to be approximately 1300 EUR/ha with respect to the standard practice of planting spruce for the entire stand (Table 2). The optimal tree species selection is virtually always "pine for the entire stand," and therefore these benefit results are independent of the microstand delineation approach. The distribution of the BLV gains is fully on the positive side, and there is possibly a weak positive trend with respect to the temperature sum, as shown for "DBSCAN, average" in Fig. 10.

On OMT sites, the mean gain in BLV is positive but depends strongly on the delineation method (Table 2). The mean gain drops from approximately 800 to 400 EUR/ha as the fraction of the infected area of the total stand area increases from approximately 0.34 to 0.69. This is because the optimal tree species selection here is "pine for the infected areas, spruce elsewhere," and the larger the share of infected area of the entire stand, the less area is left for the highly productive spruce in the healthy region (Fig. 4), and the closer the overall BLV in terms of EUR/ha for the stand drops to that of pine. Negative benefit values in the distribution are due to "spruce for the entire stand" being the optimal solution in free optimization on OMT in many cases (Table 1). There appears to be no clear trend in the BLV gain as a function of temperature sum, as is seen for "DBSCAN, average" in Fig. 10.

When maximizing net CO_2 removals and requiring eradication of root rot, the mean gain in CO_2 removals with respect to regenerating with spruce only is negative on both MT and OMT sites, for all delineation approaches (Table 2). This reflects the simulation results, which show that spruce stands are strong binders of carbon even when infected (Fig. 4). The explanation for this lies mainly in that the management of infected spruce stands entails less thinnings than usual, which leads to a high overall volume of wood in these stands.

For MT sites, the histogram of benefits in net CO_2 removals has a

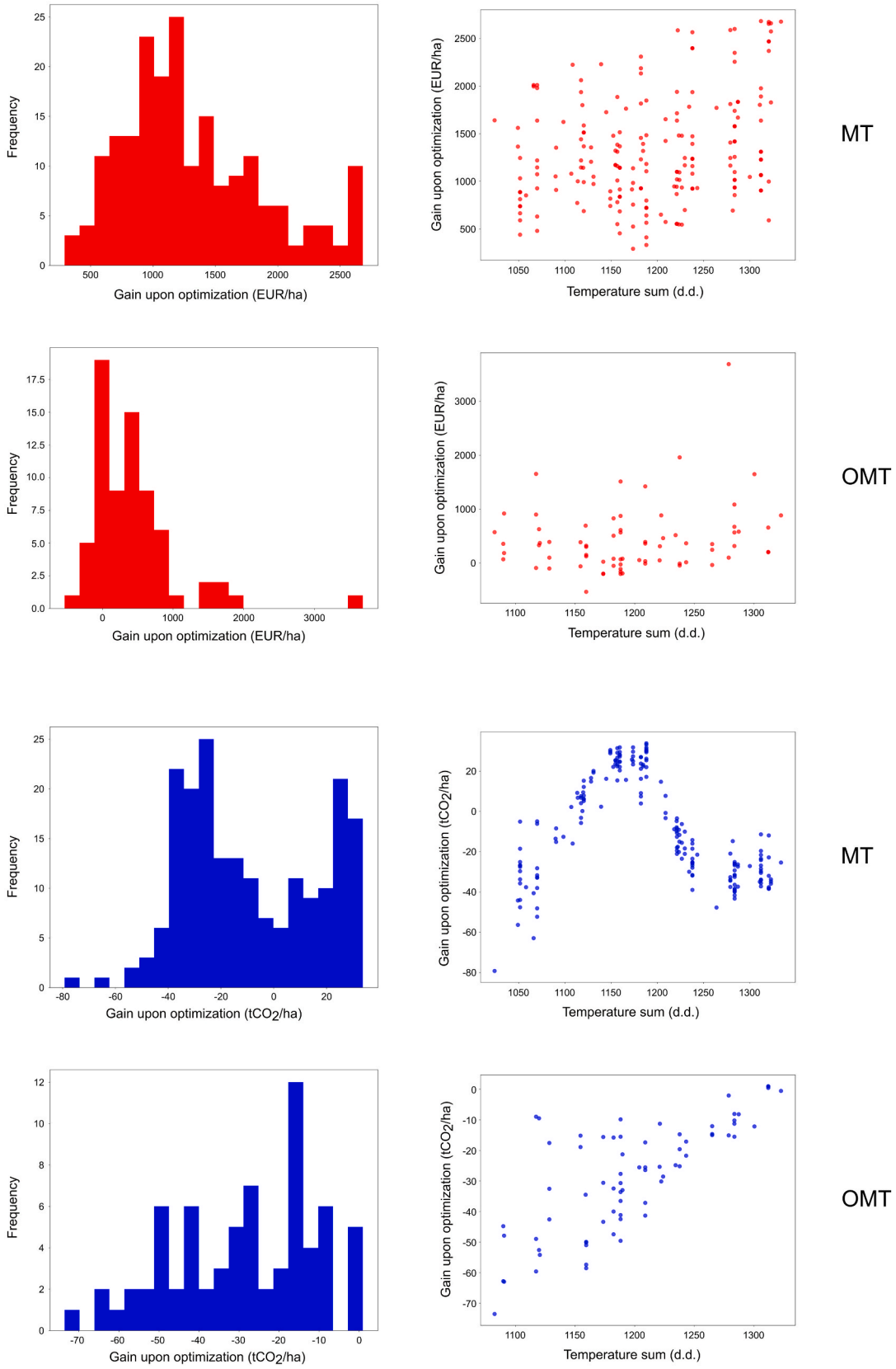

Fig. 10. Benefits of the optimization, when requiring eradication of root rot, with respect to regenerating each stand using only spruce. The benefits are given as histograms and as a function of temperature sum for BLV (red) and net CO_2 removals (blue) for the "DBSCAN, average" delineation approach. A positive gain means higher BLV or higher net CO_2 removals for the optimized solution as compared to using spruce only. The results are given separately for the two studied site types (mesic heath (MT), herb-rich heath (OMT)). The BLV results are for the case of maximizing BLV, the CO_2 results are for the case of maximizing net CO_2 removals.

Table 2
Difference in the BLV and net CO_2 removals of the optimal solution, when requiring eradication of root rot upon regeneration, with respect to the "all-spruce" solution. The BLV results are for the case of maximizing BLV, the CO_2 results are for the case of maximizing net CO_2 removals. The mean of the share of the total infected area out of the total stand area on OMT sites is given also. The error is the standard error of the mean.

	Bayes, no imputing	Bayes, with imputing	DBSCAN, fragmented	DBSCAN, average	DBSCAN, broad
Ratio of infected area to total stand area (OMT sites)	0.34 +- 0.02	0.41 +- 0.03	0.53 +- 0.02	0.64 +- 0.03	0.69 +- 0.03
Mean gain in BLV, MT (EUR/ha)	1320 +- 40	1320 +- 40	1320 +- 40	1320 +- 40	1320 +- 40
Mean gain in BLV, OMT (EUR/ha)	810 +- 70	710 +- 60	560 +- 70	420 +- 70	360 +- 80
Mean gain in CO_2 removals, MT (tCO_2/ha)	−3.9 +- 1.5	−5 +- 2	−7 +- 2	−9 +- 2	−10 +- 2
Mean gain in CO_2 removals, OMT (tCO_2/ha)	−15.6 +- 1.5	−19 +- 2	−24 +- 2	−29 +- 2	−31 +- 2

notable positive contribution (Fig. 10), which originates from the temperature sum region of approximately 1100 to 1200 d.d. where "pine for the entire stand" is the optimal solution even in free optimization (Fig. 4, Fig. 9). For other temperature sums, "spruce for the entire stand" is the optimal solution in free optimization, leading to the negative gains, i.e., losses in terms of net CO_2 removals.

On OMT sites, the histogram of benefits is practically fully on the negative side, but there is a clear positive trend in the CO_2 benefit results with growing temperature sum (Fig. 10). This is because the advantage of spruce over other tree species shrinks as the temperature sum grows (Fig. 4). However, for almost all stands (95.8%), "spruce for the entire stand" is the optimal tree species in free optimization, leading to the negative CO_2 gains, i.e., losses when requiring cleansing of the stand.

3.3.2. Benefits with respect to regenerating with the best single-species solution

Comparing the optimized solutions to planting the entire stand with spruce is interesting because the "all-spruce" solution is largely the established default solution in Finland on both MT and OMT sites. However, it is also of interest to compute the optimization benefits with respect to the best single-species solution for the entire stand, when requiring purification of the stand, as this reflects how much benefit the splitting of the stand into the healthy and infected microstands brings. For BLV optimization on MT, these gains with respect to the best single-species choice vanish for all delineation methods, because the optimal solution is "pine for the entire stand," a single-species solution itself. On OMT sites, the gains run from approximately 900 EUR/ha to 400 EUR/ha as the share of infected area of the entire stand increases from approximately 0.34 to 0.69, i.e., when the delineation method goes from "Bayes, no imputing" to "DBSCAN, broad." For net CO_2 removal optimization, the mean gain is approximately 5 to 11 tCO_2/ha on MT sites and 14 to 29 tCO_2/ha on OMT sites, depending on the delineation method.

3.4. The financial cost of eradicating root rot

Our results show that financially optimal forest regeneration does not always eradicate root rot from infected stands, as "all-spruce" is the strongest choice financially in free optimization on many OMT sites (Fig. 9). It is therefore interesting to estimate the financial cost of the eradication on our validation set (Section 2.7), i.e., the difference in the BLV between the financially optimal regeneration plan and the financially best regeneration plan that cleanses the site of root rot disease. On MT sites, the difference in mean BLV between the optimal solution in free optimization and the best solution when requiring eradication is 0 EUR/ha, as on MT sites, the economically optimal regeneration always eradicates root rot. However, on OMT type sites, this difference ranges from 0 to 57 EUR/ha over the different delineation methods, as the ratio of the infected area to the total stand area increases.

4. Discussion

The regeneration of a forest stand infected by *H. parviporum* is a challenging task in forest management. To tackle this issue, we created an optimization pipeline to guide the planning of the regeneration in terms of tree species selection and the spatial distribution of seedlings within a stand. By running our method on a set of 269 recently harvested stands in Finland, we assessed the variety of tree species recommendations and the financial and carbon-wise benefits produced by our method. We also probed the effect of varying the approach to delineating infected and healthy areas within a stand on the optimized recommendations and benefits of the optimization. Our results highlight the complex nature of the problem and demonstrate the need for decision support to guide the regeneration of infected stands. In the following, we discuss our results and their impact, considerations when applying our optimization method, and give suggestions for future work on this topic.

4.1. Tree species recommendations and benefits of using the method

In our method, the optimal regeneration plan, i.e., recommendation is produced subject to the condition that root rot is eradicated from the site. The "free optimization" approach, in which this constraint is not present, was done only for purposes of understanding the functioning of the optimization method and the results that it produces (Sections 3.2, 3.3, and 3.4).

In terms of optimal tree species to plant upon regeneration, the recommendations produced by our method are straightforward when optimizing BLV. The recommendation for MT sites is to plant pine for the entire stand, whereas the recommendation for OMT sites is to plant pine into the infected areas and spruce elsewhere. When maximizing the net CO_2 removals by the living tree biomass of the stand, the recommended choice of species is dictated by the temperature sum. The solutions then consist of pine, spruce, and birch in various configurations. These recommendations of tree species selection are independent of the chosen approach to delineating the healthy and infected microstands, for both MT and OMT.

When maximizing BLV, following the optimized recommendations brings significant financial gains on both MT and OMT sites with respect to regenerating with spruce only. Comparison of the financially optimal BLV in "free optimization" with the highest attainable BLV when requiring root rot eradication shows that the "cost" of cleansing the stand of root rot is negligible (Section 3.4).

When optimizing net CO_2 removals, i.e., total living tree biomass carbon stock, following the optimized regeneration plans brings small but consistent losses instead of gains in CO_2 removals. An exception to this is the case of intermediate temperature sums of approximately 1100 to 1200 d.d. on MT sites, where planting pine for the entire stand is the recommended solution. The explanation for the absence of CO_2 gains in the optimized results lies in the competitiveness of current management

best practices for spruce in terms of carbon accumulation, where spruce stands are grown dense and with one thinning only (Äijälä et al. 2019). However, our result of carbon losses when eradicating root rot from the stand may well be overturned when including the following wider considerations.

First, when computing the carbon content of trees based on the Motti+Hmodel simulations, carbon losses due to the wood material decaying because of root rot disease are not included, which means our net CO_2 removal results for infected spruce are somewhat overestimated. Second, root rot in spruce increases the risk of other forest damages, such as wind damage (Oliva et al. 2008, Honkaniemi et al. 2018) and mortality due to *Ips typographus* (Wahlman 2024), which makes the tree biomass carbon storage less stable. Third, rotten logs from infected stems will be used for pulp or energy wood instead of sawlogs, which may weaken the climate benefits of forest utilization. Fourth, only the carbon content of living tree biomass is considered in our analysis. Soil carbon may have a significant effect on the total carbon balance, although the direction of this effect may depend on the time span considered. Incorporating these four considerations into the analysis might well show that in comparison to growing healthy stands, growing stands suffering from Heterobasidion root rot is detrimental from the viewpoint of net CO_2 removals.

Moreover, forests are facing new growth conditions in the warming climate, including the increasing occurrence of summer droughts across Europe (Venäläinen et al. 2022). Dry conditions will favor spruce bark beetle outbreaks (Venäläinen et al. 2022), and drought together with bark beetle damage may constitute a significant cause of tree mortality, especially in spruce-dominated stands (Junttila et al. 2024). To maintain tree vigor despite these challenges, one should attempt to limit other factors of stress, such as Heterobasidion root rot.

A more straightforward approach would be to simply reduce the use of spruce and favor other tree species, and create mixed species stands and landscapes instead (Griess and Knoke 2011, Pretzsch et al. 2013, Jactel et al. 2017). Our results for optimizing BLV on MT sites recommend avoiding spruce and using pine instead. Also, many of our realized recommendations entail more than one tree species, with solutions for maximizing net CO_2 removals often including birch. When requiring eradication of root rot, our approach of splitting the stand into microstands and considering different tree species for the different microstands is predicted to bring significant gains in BLV and net CO_2 removals with respect to regenerating the entire stand with a single tree species. Favoring pine and broad-leaved trees at the expense of spruce and diversifying the tree species composition appears a sound strategy for the future. As illustrated by these results, our optimization method can clearly support this effort.

4.2. Comparison to previous work

Aza et al. (2022) proposed a precision-forestry approach for optimizing the regeneration of stands suffering from Heterobasidion root rot. One difference to our work is that in Aza et al. (2022), the stand was broken down into pixels of 16 m by 16 m in size, each with its own fertility index and rot fraction. They then chose the optimal tree species for each pixel, optimizing the entire stand regeneration, including the length of the rotation period, to maximize the BLV of the stand. Similarly to Aza et al. (2022), we find that spruce can be the optimal choice at low rot levels (Section 3.2, Fig. 9). As candidate tree species, we considered birch and a spruce-birch mixture in addition to spruce and pine, but spruce and pine consistently ended up as the winning choices in maximizing BLV. The mean gain in BLV with respect to the best single-species solution when doing "free optimization" using our method, i.e., not requiring cleansing of the stand, is 0% on the MT sites and 3 to 8% on the OMT sites of our validation set, depending on the delineation approach. Over all the sites pooled, the mean gain in BLV is approximately 1 to 2%, depending on the delineation approach. This is of the same order but somewhat lower than the 6% reported by Aza et al. (2022). Considering that the optimization in our work is more coarse-grained spatially, this can be expected.

However, fine-grained regeneration plans, involving units as small as grid cells of 16 m by 16 m, may be difficult to realize in practice. Also, in our approach, the eradication of root rot disease from the stand is the precondition for the optimization when providing the regeneration recommendation to the forest owner. Segmenting out the entire infected area from the stand is an attempt to accomplish this with confidence. In contrast, with a pixel-based approach, the peril exists that one plants spruce in an originally healthy pixel which is next to an infected pixel, and then the healthy pixel becomes infected during the rotation period. Choosing a larger pixel size might be a means to control the infection risk from neighboring pixels.

Lara et al. (2024) recently analyzed the clustering of diseased spruce trees and discussed the prospect of using harvester-based stump positioning and rot data for planning regeneration to manage root rot disease. The single-stump delineations they envision, into which to plant species resistant to root rot disease, qualitatively resemble the DBSCAN delineations given by our method at the limit of treating each infected stump as an outlier. Whereas we set the radius, i.e., buffer of our DBSCAN delineations based on considerations of stump positioning accuracy and earlier experimental work (Piri 2003), Lara et al. (2024) propose using the size of the estimated tree clusters to guide setting of the buffer size. This approach could in principle be used to tune the buffer size separately for each stand, given the harvester data on the felled trees.

4.3. Choosing and tuning the delineation method

We assume in the calculations of the total BLV or maximum net CO_2 removals by the stand that in the area delineated as "healthy," the next generation of spruce trees can grow practically free of root rot (Section 2.6). However, as the Bayes approach with imputing shows, this may not always be the case with the DBSCAN approach, which operates solely on the sawlog-sized spruce trees identified as rotten in the harvester data (Fig. 8). Therefore, the BLV results of the DBSCAN approach on OMT sites in Table 2 should be considered somewhat optimistic. Furthermore, the corresponding Bayes results on OMT sites in Table 2 should be considered somewhat optimistic, because the mean error of 4 m between the recorded and true position of the stumps (Section 2.3.1) is currently not taken into account in the modeling, and this uncertainty would likely increase the size of the infected area delineations in the Bayes approach.

Still, through offering a quantitative approach to predicting future infection risk (Section 2.3.2), and when taking into account the unknown infection states of spruce stumps, the Bayes approach with imputing could be used to produce highly optimized stand delineations with very low risk of infection in the next generation of trees. Using the DBSCAN delineations may put the next generation of spruce trees at risk of infection, because the method considers only the sawlog-sized spruce stumps identified as rotten in the harvester data.

However, increasing the area of the infected microstand delineations by varying the DBSCAN parameters might be considered a way of reducing the risk of infection from the known rotten stumps. Moreover, the DBSCAN approach is transparent and simple to run. The overall smoother DBSCAN delineations may also be more realistic to implement in practice when planting the new generation of trees.

4.4. Guiding the forest owner

In addition to the recommended choice of tree species and the microstand delineations, i.e., the optimal regeneration plan, our method outputs the BLV and maximum of the net CO_2 removals for each of the 10 regeneration alternatives (Fig. 11). This is potentially useful in guiding the decision-making of forest owners and managers. First, this allows the user to gauge, e.g., the predicted gain or loss in terms of BLV

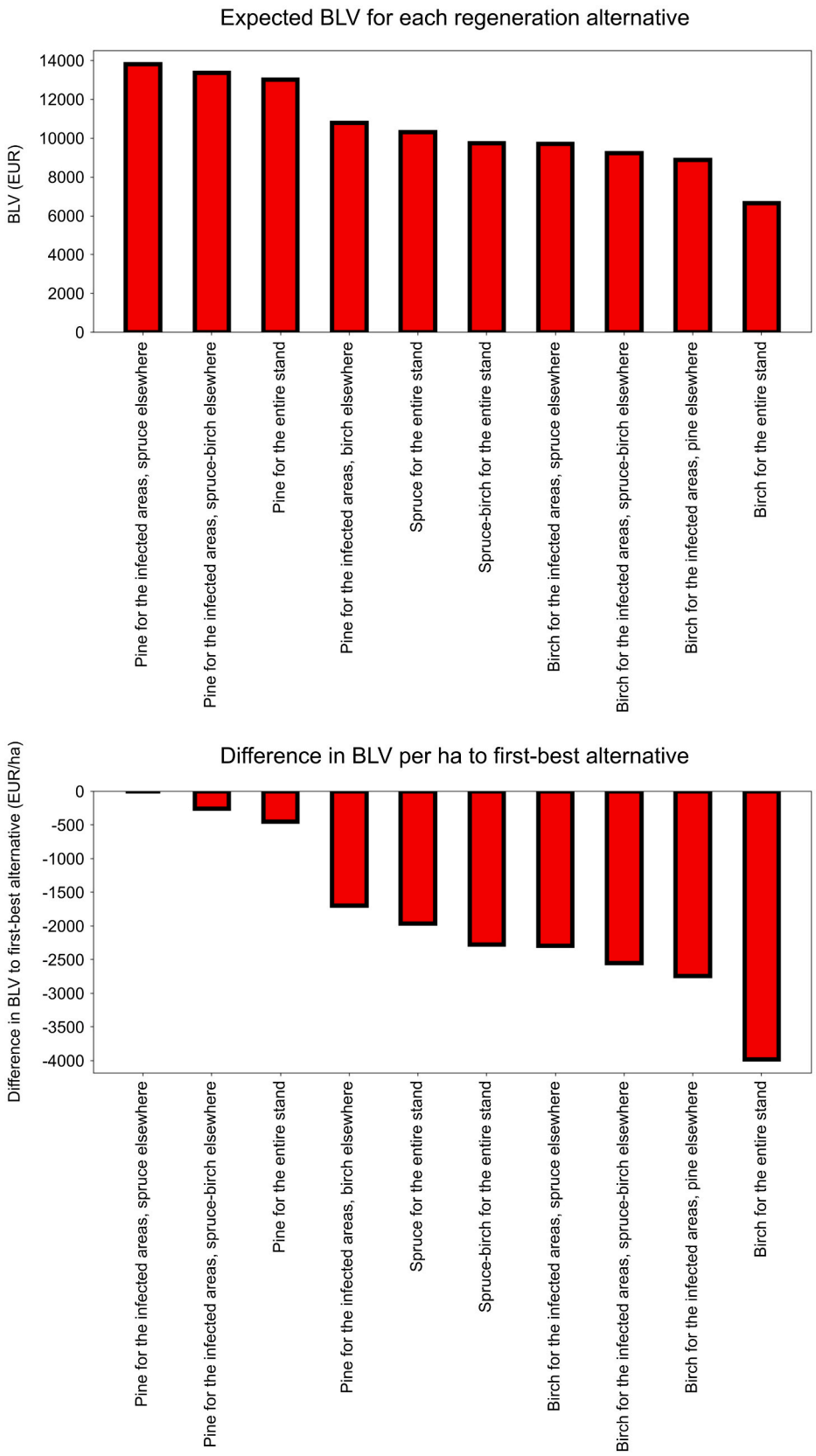

Fig. 11. The BLV results for the 10 regeneration alternatives for an example stand ($f_{rot} = 0.35$, $T_{sum} = 1237.8$ d.d., site type OMT, total stand area 1.80 ha, delineation method "DBSCAN, average"). Top: The absolute BLV results (EUR). Bottom: The difference (in EUR/ha) of the BLV of each regeneration plan to the plan with the highest BLV.

or CO_2 removals when choosing the recommended option in place of the largely established approach of regenerating the entire stand using spruce.

Second, having access to the full set of BLV results allows considering the effect of wood quality in choosing the regeneration plan. The BLV calculations (Fig. 11) are based on the volume and dimensions of logs that can be produced from the stems and the realized bulk prices (EUR/m^3) for pulp and sawlogs representing the years 2011–2020 in Finland. This means that the effect of wood quality, e.g., knottiness, is not considered when predicting the BLV for a given tree species, although in the current system, quality does have some impact on sawlog pricing. Therefore, the BLV values for, e.g., pine planted onto an OMT site are likely somewhat overestimated in our results. When considering a recommended solution that contains pine on an OMT site, such as in the case of BLV optimization, the forest owner can estimate whether the drop in price due to decreased wood quality, as realized 50–70 years into the future, will be enough to push the financial result of the pine solution below one containing, e.g., birch. In this way, the recommended regeneration plan may be fine-tuned by the user.

Third, the full set of BLV or CO_2 results may be used to answer questions such as how much would it cost (in terms of BLV or net CO_2 removals) to use, e.g., a spruce-birch mixture instead of spruce in a given spatial solution. Or how much would the cost of using birch instead of pine be when cleansing the infected areas. The boost in biodiversity when adding broad-leaved trees to the tree species distribution of the stand could then be given an estimated price.

4.5. Practical considerations

Our optimization method assumes that *H. parviporum* is the only pathogen present at the site. When applying our method in practice, should the observed root rot be caused by Armillaria spp. or *Stereum sanguinolentum*, their effect would be to increase the infected microstand areas and subsequently to reduce the area for planting spruce, a reasonable strategy in the long term (Section 4.1). Should there be *H. annosum* s.s. present at the site, we recommend regenerating the stand using birch only.

In addition to *H. annosum* s.s., the possibility of other pine-infecting pathogens on fertile sites should be kept in mind. One should also assess the actual fertility class and soil type as well as the topographical features of the stand, along with the within-site variation of wetness. Moreover, on sites that are plagued by several different disturbances, e.g., wind and insects in addition to root rot, the harvester-based estimation of the rot status of the trees may not be reliable. Furthermore, a large local moose population may prohibit the planting of birch. And while stump treatment to prevent new infections by *Heterobasidion* spores is legally obligatory during the risk period in Finland, a generally large level of infections in the broader region and consequently a high spore load may pose a risk for planting spruce. This is because thinnings introduce the possibility for new infections if stump treatment is done imperfectly in such areas. For these reasons, applying our method in practice to guide the regeneration of a stand always requires expert evaluation of the feasibility of the recommended plan on-site.

Implementing the microstand setups recommended by our method may require seedlings in different proportions of tree species than what is normally available from producers. For instance, when maximizing BLV on OMT sites, the mean fraction of pine seedlings out of all provided seedlings would be around 50% (Fig. 9, Table 1), the rest of the seedlings being spruce. The actual rot status of the previous generation of spruce trees is revealed only after the harvest, which is late in terms of changing the species composition of the seedlings for the regeneration to any notable degree. However, predictive root rot risk maps (Suvanto et al. in review) could be used to indicate the likely need for other tree species besides spruce well in advance of harvesting a stand. Regardless, in the long term, a more responsive seedling market would be helpful and perhaps even necessary for this and many other precision-forestry applications.

Another aspect of applying our method in practice is related to economies of scale: one might argue that planting microstands instead of a whole stand is more costly since smaller quantities of different seedlings (i.e., tree species) are required for an area which could have been planted with a large quantity of seedlings consisting of merely one tree species (see Rautio et al. 2023 for a discussion on the costs of artificial regeneration). This could shrink interest in our method. On the other hand, the financial benefit of applying our method was eminent (400 to 1300 EUR/ha), thus leaving some "reserve" for increased costs due to planting scattered microstands. Moreover, our method provides well-grounded guidelines for establishing mixed stands, which might otherwise be established on a more ad hoc basis. Planting with microstands entails proactive planning, but the process could probably be cost-efficiently merged into the existing forest planning environment.

4.6. Future work and extending the scope of the method

When estimating the value of different regeneration alternatives from the viewpoint of climate change mitigation, the entire lifespan of the wood, the stability of the tree biomass carbon stock with respect to damage by wind and *Ips typographus*, and the soil carbon stock should be considered for more accurate results. In addition, the lower carbon content per volume of rotten wood compared to healthy spruce wood should be taken into account in the modeling. These steps would provide a more realistic comparison of different regeneration plans in terms of climate effects.

When computing BLV in the present approach, a stand is permanently established with the chosen regeneration plan for an infinite series of rotation periods. However, after cleansing the site of root rot disease, planting spruce for the entire site, now free of root rot, will be the financially optimal choice for all OMT sites and for some MT sites. Such chains of regeneration plans could be even better performers in terms of BLV and climate change mitigation than the ones presented in this study.

We have built and validated our method for optimizing the regeneration of spruce-dominated stands infected by *H. parviporum* on data from Finland. Extending our approach to other Nordic countries should be straightforward to achieve by replacing the BLV and carbon estimates (per ha) for spruce, pine, and birch with their local versions. When moving beyond the Nordic countries, one should first map the predominant local tree species and their susceptibility to *H. parviporum* (Garbelotto & Gonthier 2013) in formulating the different regeneration alternatives, and then produce the required BLV and carbon estimates (per ha). Other pathogens of the species complex *H. annosum* s.l., which all show the same vegetative mechanism of secondary infections (Garbelotto & Gonthier 2013), could also be tackled using our approach, provided again that local tree species variety and susceptibility are considered when forming the alternative regeneration plans and estimates of BLV and carbon (per ha).

Finally, to take our optimization method into use as a decision support tool for forest owners, a more user-friendly user interface in place of the current one based on the command line may be required.

5. Conclusions

We introduced a precision-forestry method for optimizing the regeneration of spruce-dominated forest stands suffering from root rot caused by *H. parviporum* in Finland. The method aims at eradication of the disease from the site and either high financial or climate change mitigation value for the forest owner. The method uses harvester-based data on the disease status of felled spruce stems to map the positions of infected stumps at the time of clearcut. We consider both a purely spatial approach identifying known disease centers, as well as a probabilistic approach predicting future infection risk to delineate the stand into infected and healthy microstands. An extensive set of simulations of

forest and *Heterobasidion* dynamics is then used to find the best choice of tree species for each microstand to achieve either the highest BLV or net CO_2 removals, under the requirement that the stand is purified of root rot. Our method provides a novel way of controlling root rot disease while bringing financial gains to the forest owner. Due to recommended management practices for infected spruce forests, the overall CO_2 removals when using species different from spruce is often slightly lower. However, this should be reassessed after considering the forest carbon stock stability, soil carbon, and the full lifespan of the harvested wood. Through offering optimized solutions with microstands of different tree species and avoiding root rot in spruce, our method constitutes a tool for diversifying forestry and improving the resilience of forests to a range of disturbances. The approach could be extended beyond Finland and *H. parviporum* with reasonable effort. Our work is an important step in linking a new type of field data to practical forestry planning. An open-source implementation of the method is provided to enable integration with existing forestry planning systems.

Funding sources

This work was supported by the TyviTuho project funded by the Ministry of Agriculture and Forestry of Finland through the Catch the carbon research and innovation program [funding decision VN/5206/2021]. Co-funding from the Academy of Finland's Flagship Programme project UNITE – Forest-Human-Machine Interplay – Building Resilience, Redefining Value Networks and Enabling Meaningful Experiences [grant numbers 337655, 357909, and 359174] is acknowledged.

CRediT authorship contribution statement

Eero Holmström: Writing – review & editing, Writing – original draft, Visualization, Software, Project administration, Methodology, Investigation, Formal analysis, Data curation. **Juha Honkaniemi:** Writing – review & editing, Validation, Methodology. **Anssi Ahtikoski:** Writing – original draft, Validation, Methodology, Investigation, Formal analysis, Conceptualization. **Tuomas Rajala:** Writing – original draft, Visualization, Software, Methodology, Investigation, Formal analysis, Data curation, Conceptualization. **Jarkko Hantula:** Writing – review & editing, Validation, Conceptualization. **Tuula Piri:** Writing – review & editing, Validation, Conceptualization. **Juha Heikkinen:** Writing – review & editing, Validation, Methodology. **Susanne Suvanto:** Writing – review & editing, Validation, Methodology, Data curation. **Tapio Räsänen:** Writing – original draft, Validation, Methodology. **Juha-Antti Sorsa:** Writing – original draft, Validation, Methodology, Formal analysis, Data curation. **Kirsi Riekki:** Writing – original draft, Validation, Methodology, Formal analysis, Data curation. **Henna Höglund:** Writing – review & editing, Validation, Investigation, Conceptualization. **Aleksi Lehtonen:** Writing – review & editing, Validation, Conceptualization. **Mikko Peltoniemi:** Writing – review & editing, Validation, Supervision, Project administration, Methodology, Funding acquisition, Conceptualization.

Declaration of competing interest

The authors declare that they have no known competing financial interests or personal relationships that could have appeared to influence the work reported in this paper.

Acknowledgements

The authors thank Juho Kokkonen for fruitful discussions. E.H. wishes to thank Hannu Salminen and Mika Lehtonen for helpful discussions on the temperature sum data. E.H. wishes to thank CSC – IT Center for Science, Finland, for computational resources.

Appendix A. Supplementary data

Supplementary data to this article can be found online at https://doi.org/10.1016/j.compag.2025.110134.

Data availability

We make our code openly available along with a small sample of example data.

References

Ahtikoski, A., Honkaniemi, J., Holmström, E., Peltoniemi, M., 2024. Optimal species composition for stand establishment in root-rot infected forest areas. New Forests 1–14.

Ahtikoski, A., Hökkä, H., 2019. Intensive forest management—does it pay off financially on drained peatlands? Canadian Journal of Forest Research 49 (9), 1101–1113.

Aza, A., Kallio, A.M.I., Pukkala, T., Hietala, A., Gobakken, T., Astrup, R., 2022. Species selection in areas subjected to risk of root and butt rot: Applying Precision forestry in Norway. Silva Fennica 56 (3).

Bellock, K., E. (2024). The alphashape Python package. https://pypi.org/project/alphashape/.

Cappellari, M., McDermid, R.M., Alatalo, K., Blitz, L., Bois, M., Bournaud, F., Young, L. M., 2013. The ATLAS3D project–XX. Mass–size and mass–σ distributions of early-type galaxies: bulge fraction drives kinematics, mass-to-light ratio, molecular gas fraction and stellar initial mass function. Monthly Notices of the Royal Astronomical Society 432 (3), 1862–1893.

Finnish Forest Centre (2024). Open forest resource information on soil type and site fertility class. [Accessed 3rd April 2024]. https://www.metsakeskus.fi/fi/avoin-metsa-ja-luontotieto/aineistot-paikkatieto-ohjelmille/paikkatietoaineistot.

Garbelotto, M., Gonthier, P., 2013. Biology, epidemiology, and control of Heterobasidion species worldwide. Annual Review of Phytopathology 51, 39–59.

Griess, V.C., Knoke, T., 2011. Growth performance, windthrow, and insects: meta-analyses of parameters influencing performance of mixed-species stands in boreal and northern temperate biomes. Canadian Journal of Forest Research 41 (6), 1141–1159.

Grimm, V., Railsback, S.F., 2012. Pattern-oriented modelling: a 'multi-scope' for predictive systems ecology. Philosophical Transactions of the Royal Society b: Biological Sciences 367 (1586), 298–310.

Haapanen, M., Hynynen, J., Ruotsalainen, S., Siipilehto, J., Kilpeläinen, M.L., 2016. Realised and projected gains in growth, quality and simulated yield of genetically improved Scots pine in southern Finland. European Journal of Forest Research 135, 997–1009.

Holopainen, M., Vastaranta, M., Hyyppä, J., 2014. Outlook for the next generation's precision forestry in Finland. Forests 5 (7), 1682–1694.

Honkaniemi, J., Ojansuu, R., Piri, T., Kasanen, R., Lehtonen, M., Salminen, H., Mäkinen, H., 2014. Hmodel, a Heterobasidion annosum model for even-aged Norway spruce stands. Canadian Journal of Forest Research 44 (7), 796–809.

Honkaniemi, J., Piri, T., Lehtonen, M., Siipilehto, J., Heikkinen, J., Ojansuu, R., 2017. Modelling the mechanisms behind the key epidemiological processes of the conifer pathogen Heterobasidion annosum. Fungal Ecology 25, 29–40.

Honkaniemi, J., Ojansuu, R., Kasanen, R., Heliövaara, K., 2018. Interaction of disturbance agents on Norway spruce: A mechanistic model of bark beetle dynamics integrated in simulation framework WINDROT. Ecological Modelling 388, 45–60.

Hynynen, J., Ahtikoski, A., Siitonen, J., Sievänen, R., Liski, J., 2005. Applying the MOTTI simulator to analyse the effects of alternative management schedules on timber and non-timber production. Forest Ecology and Management 207 (1–2), 5–18.

Hynynen, J., Salminen, H., Ahtikoski, A., Huuskonen, S., Ojansuu, R., Siipilehto, J., ... & Eerikäinen, K. (2014). Scenario analysis for the biomass supply potential and the future development of Finnish forest resources.

Hynynen, J., Salminen, H., Ahtikoski, A., Huuskonen, S., Ojansuu, R., Siipilehto, J., Eerikäinen, K., 2015. Long-term impacts of forest management on biomass supply and forest resource development: a scenario analysis for Finland. European Journal of Forest Research 134, 415–431.

Jactel, H., Bauhus, J., Boberg, J., Bonal, D., Castagneyrol, B., Gardiner, B., Brockerhoff, E.G., 2017. Tree diversity drives forest stand resistance to natural disturbances. Current Forestry Reports 3, 223–243.

Junttila, S., Blomqvist, M., Laukkanen, V., Heinaro, E., Polvivaara, A., O'Sullivan, H., Peltola, H., 2024. Significant increase in forest canopy mortality in boreal forests in Southeast Finland. Forest Ecology and Management 565, 122020.

Juutinen, A., Ahtikoski, A., Lehtonen, M., Mäkipää, R., Ollikainen, M., 2018. The impact of a short-term carbon payment scheme on forest management. Forest Policy and Economics 90, 115–127.

Korhonen, K., 1978. Intersterility groups of *Heterobasidion annosum*. Commun. Inst. for. Fenn. 94 (6), 25.

Korhonen, K., Piri, T. (1994). The main hosts and distribution of the S and P groups of *Heterobasidion annosum* in Finland. In: Johansson, M. & Stenlid, J. (Eds.), Proceedings of the 8th Int. Conf. on Root and Butt Rots, Sweden and Finland, Aug. 9-16, 1993, Swedish University of Agricultural Sciences, Uppsala, Sweden, pp. 260-267. ISBN 91- 576-4803-4.

Korhonen, K., Stenlid, J., 1998. Biology of *Heterobasidion annosum*. In: Woodward, J., Stenlid, R., Karjalainen, A., Hüttermann, A. (Eds.), *Heterobasidion Annosum*: Biology,

Ecology, Impact and Control; S. London CAB International, Wallingford, UK, pp. 43–70.
Lara, W., Astrup, R., Hietala, A.M., Maleki, K., Belbo, H., Antón-Fernández, C., 2024. Mapping pathogenic fungi in decayed Norway spruce stands: Insights from harvester positional data. Journal of Applied Ecology.
Matala, J., Hynynen, J., Miina, J., Ojansuu, R., Peltola, H., Sievänen, R., Kellomäki, S., 2003. Comparison of a physiological model and a statistical model for prediction of growth and yield in boreal forests. Ecological Modelling 161 (1–2), 95–116.
Mönkkönen, M., Juutinen, A., Mazziotta, A., Miettinen, K., Podkopaev, D., Reunanen, P., Tikkanen, O.P., 2014. Spatially dynamic forest management to sustain biodiversity and economic returns. Journal of Environmental Management 134, 80–89.
Möykkynen, T., Pukkala, T., 2011. Effect of planting Scots pine around Norway spruce stumps on the spread of Heterobasidion coll. Forest Pathology 41 (3), 212–220.
Müller, M.M., Hamberg, L., Kuuskeri, J., La Porta, N., Pavlov, I., Korhonen, K., 2015. Respiration rate determinations suggest *Heterobasidion parviporum* subpopulations have potential to adapt to global warming. For. Pathol. 45 (6), 515–524.
Ojansuu, R., Henttonen, H., 1983. Lämpösumman ja sademäärän paikallisten arvojen johtaminen ilmatieteen laitoksen mittaustiedoista. Summary: Estimation of local values of monthly mean temperatures. Silva Fennica 17 (2), 143–160.
Oliva, J., Samils, N., Johansson, U., Bendz-Hellgren, M., Stenlid, J., 2008. Urea treatment reduced Heterobasidion annosum sl root rot in Picea abies after 15 years. Forest Ecology and Management 255 (7), 2876–2882.
Pedregosa, F., Varoquaux, G., Gramfort, A., Michel, V., Thirion, B., Grisel, O., Duchesnay, É., 2011. Scikit-learn: Machine learning in Python. The Journal of Machine Learning Research 12, 2825–2830.
Piri, T., 1996. The spreading of the S type of *Heterobasidion annosum* from Norway spruce stumps to the subsequent tree stand. Eur. J. for. Pathol. 26, 193–204.
Piri, T. (2003). Silvicultural control of Heterobasidion root rot in Norway spruce forests in southern Finland: Regeneration and vitality fertilization of infected stands.
Piri, T., Korhonen, K., 2001. Infection of advance regeneration of Norway spruce by *Heterobasidion parviporum*. Can. J. for. Res. 31, 937–942.
Piri, T., Korhonen, K., Sairanen, A., 1990. Occurrence of Heterobasidion annosum in pure and mixed spruce stands in southern Finland. Scandinavian Journal of Forest Research 5 (1–4), 113–125.
Pretzsch, H., Schütze, G., Uhl, E., 2013. Resistance of European tree species to drought stress in mixed versus pure forests: evidence of stress release by inter-specific facilitation. Plant Biology 15 (3), 483–495.
Rautio, P., Lideskog, H., Bergsten, U., Karlberg, M., 2023. Perspectives: Lean forestry–A paradigm shift from economies of scale to precise and sustainable use of ecosystem services in forests. Forest Ecology and Management 530, 120766.
Repola, J., 2008. Biomass equations for birch in Finland. Silva Fennica 42 (4), 605–624.
Repola, J., 2009. Biomass equations for Scots pine and Norway spruce in Finland. Silva Fennica 43 (4), 625–647.
Stenlid, J., Wästerlund, I., 1986. Estimating the frequency of stem rot in *Picea abies* using an increment borer. Scand. J. for. Res. 1 (1–4), 303–308.
Suvanto, S., Heikkinen, J., Honkaniemi, J., Holmström, E., Piri, T., Hantula, J., Rajala, T., Räsänen, T., Riekki, K., Sorsa, J.-A., Hytönen, H., Höglund, H., Lehtonen, A., Peltoniemi, M. Rot or not? Uncovering the spatial patterns and drivers of Norway spruce root rot with harvester data. In review. Preprint available at https://doi.org/10.1101/2025.02.07.637055.
Taipale, E., Riekki, K., Melkas, T., & Malinen, J. Hakkuupään sijaintitiedon tarkkuus. Metsätehon tuloskalvosarja 1/2022. https://www.metsateho.fi/hakkuupaan-sijaintitiedon-tarkkuus/ (In Finnish).
Venäläinen, A., Ruosteenoja, K., Lehtonen, I., Laapas, M., Tikkanen, O.P., Peltola, H., 2022. Climate change, impacts, adaptation and risk management. In: Forest Bioeconomy and Climate Change. Springer International Publishing, Cham, pp. 33–53.
Wahlman, W. (2024). The effect of Heterobasidion root rot on *Ips typographus* infestation risk on Norway spruce. Master's thesis. University of Helsinki, 2024. Available at https://helda.helsinki.fi/server/api/core/bitstreams/3fb8baff-1edb-41c2-b842-97cc4624f4a4/content.
Woodward S, Stenlid J, Karjalainen R, Hüttermann A. Preface. In: Woodward S, Stenlid J, Karjalainen R, Hüttermann A, editors. Heterobasidion Annosum Biol. Ecol. Impact Control. Wallingford: CABI; 1998. p. xi–xii.
Äijälä, O., Koistinen, A., Sved, J., Vanhatalo, K., Väisänen, P., 2019. Metsänhoidon suositukset [Silvicultural recommendations]. The Forestry Development Centre Tapio, Helsinki, Finland. In Finnish.